VOL.32 NO.1-4 2022

Research Alert

CSIR–SERC
ENGINEERING SUSTAINABLE STRUCTURES

KNOWLEDGE RESOURCE DIVISION
CSIR-STRUCTURAL ENGINEERING RESEARCH CENTRE
TARAMANI, CHENNAI 600113

TABLE OF CONTENTS

RESEARCH PAPERS FROM JOURNALS

Construction and Building Materials

2022/1
A typical adsorption of polycarboxylate superplasticizers on calcium silicate hydrate surface: Converting interaction by solvent effects
Hou, D.; et al.
Vol. 330, Article No. 127160, May 2022

2022/2
Enhanced flame retardancy of modified β-cyclodextrin doped silica fume-based geopolymeric coating covered on plywood
Wang, Y.; et al.
Vol. 330, Article No. 127231, May 2022

2022/3
Sustainable clinker-free solid waste binder produced from wet-ground granulated blast-furnace slag, phosphogypsum and carbide slag
Yang, J.; et al.
Vol. 330, Article No. 127218, May 2022

2022/4
Effects of citrate acid, solidum silicate and their compound on the properties of magnesium oxysulfate cement under carbonation condition
Sun, Q.; et al.
Vol. 330, Article No. 127316, May 2022

2022/5
Self-healing performance and prediction model of microcapsule asphalt
Li, J.; et al.
Vol. 330, Article No. 127085, May 2022

2022/6
Mechanical properties and electromagnetic absorption characteristics of foam Cement-based absorbing materials
Bai, Y.; et al.
Vol. 330, Article No. 127221, May 2022

2022/7
Codes applicability of estimating the FRC compressive strength by the core-drilling method
Taman, M.; Abd Elaty, M.; Behiry, R. N.
Vol. 330, Article No. 127227, May 2022

2022/8
Modification of self-cleaning activity on cement pastes containing nano-TiO2 due to CO2 curing
Moro, C.; et al.
Vol. 330, Article No. 127185, May 2022

2022/9
Feasibility assessment of CeO2 nanoparticles as aging-resistant agent of asphalt
Zhao, Z.; et al.
Vol. 330, Article No. 127245, May 2022

2022/10
Exemplification of sustainable sodium silicate waste sediments as coarse aggregates in the performance evaluation of geopolymer concrete
Kanagaraj. B.; et al.
Vol. 330, Article No. 127135, May 2022

2022/11
Upcycle olive pomace as antioxidant and recycling agent in asphalt paving materials
Zhang, K.; Zhao, H.; Wang, S. C.
Vol. 330, Article No. 127217, May 2022

2022/12
Interlayer bonding investigation of 3D printing cementitious materials with fluidity-retaining polycarboxylate superplasticizer and high-dispersion polycarboxylate superplasticizer
Pan, T.; Jiang, Y.; Ji, X.
Vol. 330, Article No. 127151, May 2022

2022/13
A 14-year study on ceramic waste slag-based lightweight aggregate concrete
Liang, Y.; et al.

Vol. 330, Article No. 127152, May 2022

2022/14
Enhanced mechanical properties of polymer-modified cementitious materials via organosilane fly ash hybrid–polyvinyl pyrrolidone crosslink network
Zhao, D.; et al.
Vol. 330, Article No. 127119, May 2022

2022/15
Utilization of micro encapsulated phase change material in asphalt concrete for improving low-temperature properties and delaying black ice
Phan, T. M.; Park, D.; Kim, H.
Vol. 330, Article No. 127262, May 2022

2022/16
Pore characteristics and permeability simulation of porous asphalt mixture in pouring semi-flexible pavement
Ling, S.; et al.
Vol. 330, Article No. 127253, May 2022

2022/17
Size effect of ultra-high-performance concrete under compression: effects of steel fiber characteristics and water-to-binder ratio
Zhang, C.; et al.
Vol. 330, Article No. 127170, May 2022

2022/18
Effect of secondary curing on the performance of microwave cured concrete
Zhou, F.; et al.
Vol. 330, Article No. 127256, May 2022

2022/19
Study on curing characteristics of cold-mixed and cold-laid asphalt mixture based on electrical properties
Xu, W.; et al.
Vol. 330, Article No. 127223, May 2022

2022/20
Multi-factor sensitivity analysis of chloride ingression: A case study for Hangzhou Bay Bridge
Song, L.; et al.
Vol. 330, Article No. 127089, May 2022

2022/21
You only design once (YODO): Gaussian Process-Batch Bayesian optimization framework for mixture design of ultra-high performance concrete
Saleh, E.; et al.
Vol. 330, Article No. 127270, May 2022

2022/22
Understanding the effects of mix proportion parameters on the dynamic stability of ground limestone mortar based on the velocity of particle and paste film thickness
Zhang, Z.; et al.
Vol. 330, Article No. 127246, May 2022

2022/23
A bi-block sleeper dynamic strain monitoring method based on embedded FRP-OF sensor
Li, P.; et al.
Vol. 330, Article No. 127271, May 2022

2022/24
Three-dimensional mesostructure model of coupled electromagnetic and heat transfer for microwave heating on steel slag asphalt mixtures
Luo, W.; et al.
Vol. 330, Article No. 127235, May 2022

2022/25
Modifying effect of anionic polyacrylamide dose for cement-based 3DP materials: Printability and mechanical performance tests
Liu, Q.; et al.
Vol. 330, Article No. 127156, May 2022

2022/26
Pore structure change and physico-mechanical properties deterioration of sandstone suffering freeze-thaw actions
Huang, S.; et al.
Vol. 330, Article No. 127200, May 2022

2022/27
Advanced utilization of molybdenum tailings in producing Ultra High-Performance Composites based on a green activation strategy
Yu, R.; et al.
Vol. 330, Article No. 127272, May 2022

2022/28
Evaluation on the full-scale testbed performance of lightweight foamed soil using railroad loading system
Le, T. H. M.; et al.
Vol. 330, Article No. 127249, May 2022

2022/29
Mechanical properties, crack evolution and damage characteristics of prefabricated fractured cemented paste backfill under uniaxial compression
Song, X.; et al.
Vol. 330, Article No. 127251, May 2022

2022/30
Cost-effective assessment of in-service asphalt pavement condition based on Random Forests and regression analysis
Guo, W.; et al.
Vol. 330, Article No. 127219, May 2022

2022/31
Study on the strength characteristics and failure characteristics of the composite load-bearing structure in the cemented filling field
Xu, B.; et al.
Vol. 330, Article No. 127242, May 2022

2022/32
Influence of bedrock on the dynamic deflection response and dynamic back-calculation results of asphalt pavement: Insights from the numerical simulation of falling weight deflectometer tests
Wang, Y.; et al.
Vol. 330, Article No. 127252, May 2022

2022/33
Occurrence and leaching behaviors of heavy-metal elements in metallurgical slags
Pang, L.; et al.
Vol. 330, Article No. 127268, May 2022

2022/34
Synthesis of phase change microcapsules with binary fatty acid ester core and their feasibility investigation in energy conservation of cementitious materials
Ma, J.; et al.
Vol. 330, Article No. 127212, May 2022

2022/35
Experimental and numerical investigation of drying rate impact on moisture loss, exchange coefficient and drying shrinkage of cement paste
Kinda, J.; et al.
Vol. 330, Article No. 127099, May 2022

2022/36
Experimental study on high-temperature relaxation behavior of carbon fiber reinforced polymer cable
Jiamg, Z.; et al.
Vol. 330, Article No. 127207, May 2022

2022/37
Inhomogeneities of carbonation depth distributions in recycled aggregate concretes: A visualisation and quantification study
Mi, R.; Pan, G.
Vol. 330, Article No. 127300, May 2022

2022/38
Effects of hydraulic binder composition on the rheological characteristics of recycled mixtures with foamed bitumen for full depth reclamation
Iwański, M.; et al.
Vol. 330, Article No. 127274, May 2022

2022/39
Research on energy dissipation and damage evolution of dynamic splitting failure of basalt fiber reinforced concrete
Xie, H.; et al.
Vol. 330, Article No. 127292, May 2022

2022/40
Study on the mechanical characteristics and damage evaluation of concrete-rock combination after high temperatures exposure
Shen, M.; et al.
Vol. 330, Article No. 127278, May 2022

2022/41
Influence of fibers distribution on direct shear and flexural behavior of synthetic fiber-reinforced self-compacting concrete
González-Aviña, J. V.; et al.
Vol. 330, Article No. 127255, May 2022

2022/42
Thermal behavior evaluation of a radiant floor heating system incorporates a microencapsulated phase change material
Babaharra, O.; et al.
Vol. 330, Article No. 127293, May 2022

2022/43
Hybrid machine learning model and Shapley additive explanations for compressive strength of sustainable concrete
Wu, Y.; et al.
Vol. 330, Article No. 127298, May 2022

2022/44
The influence of inaccuracies in the production process on the load-bearing behaviour of timber step joints
Braun, M.; Kromoser, B.
Vol. 330, Article No. 127285, May 2022

2022/45
Gradient power modified ohmic heating curing to prepare hybrid carbon fibers/high performance concrete under deep-freeze low temperature
Ouyang, M.; et al.
Vol. 330, Article No. 127279, May 2022

2022/46
The feasibility of recycled micro polyethylene terephthalate (PET) replacing natural sand in hot-mix asphalt
Ferreira, J. W. D. S.; et al.
Vol. 330, Article No. 127276, May 2022

2022/47
Taguchi-based interval multi-criteria decision-making method for optimisation of alkali activators
Bayat, A.; Eslami, A.
Vol. 330, Article No. 127234, May 2022

2022/48
Multi-objective design optimization for graphite-based nanomaterials reinforced cementitious composites: A data-driven method with machine learning and NSGA-Ⅱ
Dong, W.; et al.
Vol. 331, Article No. 127198, May 2022

2022/49
Push-out tests on studs with UHPC cover embedded in UHPC-NSC composite slab
Yang, H.; et al.
Vol. 331, Article No. 127210, May 2022

2022/50
A study on the change in frost resistance and pore structure of concrete containing blast furnace slag under the carbonation conditions
Ding, Z.; et al.
Vol. 331, Article No. 127295, May 2022

2022/51
Effects of hydrophilic and hydrophobic nanosilica on the hydromechanical behaviors of mudstone soil
Ghadr, S.; et al.
Vol. 331, Article No. 127263, May 2022

2022/52
Fire behaviour of hemp, clay and gypsum-based light biobased concretes and renders
Sonnier, R.; et al.
Vol. 331, Article No. 127230, May 2022

2022/53
Using 3-D velocity contour plots to detect voids in grouted tendon ducts in post-tensioned concrete construction
Cheng, C. C.; et al.
Vol. 331, Article No. 127277, May 2022

2022/54
Study on dynamic response and permanent deformation of the pier and its surrounding sites induced by high-speed train loads in seasonally frozen regions
Zheng, H.; Yan, W.
Vol. 331, Article No. 127264, May 2022

2022/55
Calculation analysis method to model the creep of recycled aggregate of thermal insulation concrete
Wang, Z.; et al.
Vol. 331, Article No. 127229, May 2022

2022/56
Arresting behavior of foamed concrete used in EMAS subjected to wind erosion and wet-dry cycles
Meng, Y.; Zhang, W.; Gao, L.
Vol. 331, Article No. 127299, May 2022

2022/57
Mechanical properties evaluation of crumb rubber asphalt mixture for elastic trackbed
Wang, T.; et al.
Vol. 331, Article No. 127048, May 2022

2022/58
Effect of the incorporation of PET fiber and ternary blended binder on the flexural and tensile behaviour of ultra-high performance green concrete
Alhani, A. H.; et al.
Vol. 331, Article No. 127306, May 2022

2022/59
Clarifying the deformation restriction of unhydrated phase in cement paste to its autogenous shrinkage
Guo, Y.; et al.
Vol. 331, Article No. 127297, May 2022

2022/60
Understanding the effect of vitamin B3, B6 and C as a corrosion inhibitor on the ordinary Portland cement hydration: Experiments and DFT study
Xu, Q.; et al.
Vol. 331, Article No. 127294, May 2022

2022/61
Thermal and mechanical characterization of fly ash geopolymer with aluminium chloride and potassium hydroxide treated hemp shiv lightweight aggregate
Narattha, C.; Wattanasiriwech, S.; Wattanasiriwech, D.
Vol. 331, Article No. 127206, May 2022

2022/62
Internal curing effect of saturated coral coarse aggregate in high-strength seawater sea sand concrete
Zhou, L.; et al.
Vol. 331, Article No. 127280, May 2022

2022/63
Self-sensing fabric reinforced cementitious matrix systems for combined strengthening and monitoring of concrete structures
Shaikh, A.; Butler, L. J.
Vol. 331, Article No. 127243, May 2022

2022/64
Strength development and microstructure of recycled gypsum-soda residue-GGBS based geopolymer
An, Q.; et al.
Vol. 331, Article No. 127312, May 2022

2022/65
Physical properties, strength, and impurities stability of phosphogypsum-based cold-bonded aggregates
Ding, C.; et al.
Vol. 331, Article No. 127307, May 2022

2022/66
Dynamic load responses of perpetual pavement test roads on U.S. 23: Full-scale instrumentation and evaluation
Zhu, J.; et al.
Vol. 331, Article No. 127326, May 2022

2022/67
Electrically driven ionic transport in the RCM and RIM: Investigations based on experiments and numerical simulations
Liu, J.; et al.
Vol. 331, Article No. 127331, May 2022

2022/68
A novel anti-clay silane-modified polycarboxylate superplasticizer: Preparation, performance and mechanism
Wang, R.; et al.
Vol. 331, Article No. 127311, May 2022

2022/69
Quantifying oxygen diffusion in bitumen films using molecular dynamics simulations
Gao, Y.; et al.
Vol. 331, Article No. 127325, May 2022

2022/70
Dry shrinkage performance of cement-stabilized reclaimed lime-fly ash macadam
Sun, Y.; et al.
Vol. 331, Article No. 127332, May 2022

2022/71
Smart glazing thermal comfort improvement through near-infrared shielding paraffin incorporated SnO2-Al2O3 composite
Roy, A.; et al.
Vol. 331, Article No. 127319, May 2022

2022/72
Study on evaluation of elastic modulus of crumb rubber concrete in meso-scale
Cai, X.; et al.
Vol. 331, Article No. 127247, May 2022

2022/73
Deformation mechanism and soil evolution analysis based on different types geogrid reinforced foundation
Gao, J.; et al.
Vol. 331, Article No. 127322, May 2022

2022/74
Numerical simulation of steel corrosion in chloride environment based on random aggregate concrete microstructure model
Wang, H.; et al.

Vol. 331, Article No. 127323, May 2022

2022/75
Nano-Al2O3 composite on intermediate and high temperature properties of neat and modified asphalt binders and their effect on hot mix asphalt mixtures
Mamuye, Y.; Liao, M. C.; Do, N. D.
Vol. 331, Article No. 127304, May 2022

2022/76
Permeability evolution characteristics and microanalysis of reactive powder concrete of drilling shaft lining under stress-seepage coupling
Fang, Y.; et al.
Vol. 331, Article No. 127336, May 2022

2022/77
Experimental investigation on the interfacial shear bond performance of non-water reacting polymer and concrete
Qin, L.; et al.
Vol. 331, Article No. 127351, May 2022

2022/78
Thermo-mechanical behaviour of fly ash-ladle furnace slag blended geopolymer with incorporation of decahydrate borax
Hui-Teng, N.; et al.
Vol. 331, Article No. 127337, May 2022

2022/79
Application of zeolite as a bacterial carrier in the self-healing of cement mortar cracks
Yuan, H.; et al.
Vol. 331, Article No. 127324, May 2022

2022/80
Application of nanoindentation in asphalt material aging and characterization of actual pavement aging
Yu, Y.; et al.
Vol. 331, Article No. 127348, May 2022

2022/81
Experimental investigation of the moment-rotation behaviour of beam-column connections produced using compressed wood connectors
Mehra, S.; et al.
Vol. 331, Article No. 127327, May 2022

2022/82
Real-time monitoring of humidity inside concrete structures utilizing embedded smart aggregates
Zhang, H.; Li, J.; Kang, F.
Vol. 331, Article No. 127317, May 2022

2022/83
Investigation on the properties of epoxy asphalt mixture containing crumb rubber for bridge expansion joint
Min, Z.; et al.
Vol. 331, Article No. 127344, May 2022

2022/84
Evaluation of prestress relaxation loss and harping characteristics of prestressing CFRP systems
Tahsiri, H.; Belarbi, A.
Vol. 331, Article No. 127399, May 2022

2022/85
Assessment of the tensile behaviour of post-installed screw anchors in early age concrete
Obayes, O.; et al.
Vol. 331, Article No. 127350, May 2022

2022/86
The effect of heat treatment on the kinetics of the delayed ettringite formation – An improved chemo-thermal-hygral model
Kothari, C.; Takahashi, Y.
Vol. 331, Article No. 127358, May 2022

2022/87
Effects of retrieving powder on mechanical and shrinkage properties of vertical vibration compacted cement-stabilized macadam
Yuan, K.; et al.
Vol. 331, Article No. 127305, May 2022

2022/88
Correlation of flaw structure and cracking behavior in SHCC with X-ray CT scanning technique
Lu, C.; et al.
Vol. 331, Article No. 127296, May 2022

2022/89
Mechanical behavior of GFRP-bamboo composite shear connections
Wahan, M. Y.; et al.
Vol. 331, Article No. 127333, May 2022

2022/90
Mechanical properties of fibre reinforced seawater sea-sand recycled aggregate concrete under axial compression
Huang, Y.; et al.
Vol. 331, Article No. 127338, May 2022

2022/91
Nonlinear-elastic characterization of cement-based materials under uniaxial stress: A comparison between ultrasonic and resonance techniques
Spalvier, A.; et al.
Vol. 331, Article No. 127211, May 2022

2022/92
Properties of additively manufactured geopolymer incorporating mineral wollastonite microfibers
Bong, S. H.; et al.
Vol. 331, Article No. 127282, May 2022

2022/93
Moisture susceptibility of asphalt mixtures: 2S2P1D rheological model approach and new index based on dynamic modulus master curve changes
Brondani, C.; et al.
Vol. 331, Article No. 127316, May 2022

2022/94
Lab-scale reproduction test method for temperature-driven movement of through-thickness cracks in concrete exterior walls for crack repair evaluation
Li, Y.; et al.
Vol. 331, Article No. 127169, May 2022

2022/95
Development of strain-hardening geopolymer mortar based on liquid-crystal display (LCD) glass and blast furnace slag
Yoo, D. Y.; et al.
Vol. 331, Article No. 127334, May 2022

2022/96
Impact behaviour of fly ash and slag-based geopolymeric concrete: The effects of recycled aggregate content, water-binder ratio and curing age
Xie, J.; et al.
Vol. 331, Article No. 127359, May 2022

2022/97
The improvement of the thermal and acoustic insulation properties of phosphogypsum specimens by adding waste wood fibre
Fornés, I. V.; et al.
Vol. 331, Article No. 127341, May 2022

2022/98
Shrinkage performance of concrete for shotcrete use restrained by rock in hot and dry tunnel environment
Liu, P.; et al.
Vol. 331, Article No. 127314, May 2022

2022/99
Performance of glass powder substituted slag based geopolymer concretes under high temperature
Derinpinar, A. N.; Karakoç, M. B.; Özcan, A.
Vol. 331, Article No. 127318, May 2022

2022/100
Improvement of the dynamic failure behavior of concrete subjected to projectile impact using user-defined material model
Shin, W.; Park, H.; Han, J.
Vol. 332, Article No. 127343, May 2022

2022/101
Strength and post-freeze-thaw behavior of a marl soil modified by lignosulfonate and polypropylene fiber: An environmentally friendly approach
Vakili, A. H.; et al.
Vol. 332, Article No. 127364, May 2022

2022/102
Residual seismic capacity of beam-column components with corroded reinforcement
Opabola, E. A.
Vol. 332, Article No. 127269, May 2022

2022/103
Thermal behavior and post-heating fracture characteristics of polypropylene microfiber-reinforced geopolymer binders
Irshidat, M. R.; Al-Nuaimi, N.; Rabie, M.
Vol. 332, Article No. 127310, May 2022

2022/104
Mechanical property and microstructure development in alkali activated fly ash slag blends due to efflorescence
Srinivasamurthy, L.; et al.
Vol. 332, Article No. 127273, May 2022

2022/105
Evaluation of the fractures of asphalt concrete added with rubber particles based on the fine aggregate mixtures
Zu-yuan, L.; et al.
Vol. 332, Article No. 127365, May 2022

2022/106
Effect of fine aggregate gradation on the rheology of mortar
Li, T.; et al.
Vol. 332, Article No. 127362, May 2022

2022/107
Mechanism analysis of strength evolution of concrete structure in saline soil area based on 15-year service
Long, Z.; et al.
Vol. 332, Article No. 127281, May 2022

2022/108
Impact of rest period on asphalt concrete permanent deformation
Alrajhi, A.; Ozer, H.; Al-Qadi, I. L.
Vol. 332, Article No. 127329, May 2022

2022/109
Temperature characteristics of permeable asphalt pavement: Field research
Lu, R.; et al.
Vol. 332, Article No. 127379, May 2022

2022/110
The adaptability of Sporosarcina pasteurii in marine environments and the feasibility of its application in mortar crack repair
Fu, Q.; et al.
Vol. 332, Article No. 127371, May 2022

2022/111
Flexural toughness and compressive stress–strain behaviour of pseudoelastic shape memory alloy fibre reinforced concrete
Dehghani, A.; Aslani, F.

Vol. 332, Article No. 127372, May 2022

2022/112
Use of Hydrated Ladle Furnace Slag as a filler substitute in asphalt mastics: Rheological analysis of filler/bitumen interaction
Lagos-Varas, M.; et al.
Vol. 332, Article No. 127370, May 2022

2022/113
Pozzolanic characteristics of silica recovered from olivine
Shah, V.; Scott, A.
Vol. 332, Article No. 127378, May 2022

2022/114
Effect of fillers on the behaviour of heavy-weight concrete made by iron sand
Lai, M. H.; et al.
Vol. 332, Article No. 127357, May 2022

2022/115
Optimization of the thermal conductivity test for building insulation materials under multifactor impact
Yang, W.; Wang, Y.; Liu, J.
Vol. 332, Article No. 127380, May 2022

2022/116
Compressive mechanical properties of self-expanding grouting materials with different densities
Li, X.; et al.
Vol. 332, Article No. 127308, May 2022

2022/117
Comparative effectiveness of fibers in enhancing engineering properties of Earth as a building Material: A reviewq
Paul, S.; Islam, M. S.; Elahi, T. E.
Vol. 332, Article No. 127366, May 2022

2022/118
Wear law of Q345 steel under the abrasion–corrosion synergistic effect of cemented paste backfill
Wang, X.; et al.
Vol. 332, Article No. 127283, May 2022

2022/119
Performance-based design of asphalt pavements concerning the reliability analysis
Norouzi, Y.; et al.
Vol. 332, Article No. 127393, May 2022

2022/120
Effects of binder and aggregate properties on the permanent deformation of asphalt mixtures by means of uniaxial and triaxial tests
de Barros, L. M.; et al.
Vol. 332, Article No. 127346, May 2022

2022/121
Thermal conductivity of scrap tire rubber-sand composite as insulating material: Experimental investigation and predictive modeling
Yang, Y. L.; et al.
Vol. 332, Article No. 127387, May 2022

2022/122
Compressive behavior of double-skin tubular stub columns with recycled aggregate concrete and a PET FRP jacket
Bai, Y. L.; et al.
Vol. 332, Article No. 127321, May 2022

2022/123
Application and validation of fly ash based geopolymer mortar as grouting material in porous asphalt concrete
Bai, T.; et al.
Vol. 332, Article No. 127154, May 2022

2022/124
Rheological properties of cement paste blended with sugarcane bagasse ash and rice straw ash

Athira, G.; Bahurudeen, A.
Vol. 332, Article No. 127377, May 2022

2022/125
Strength characteristics and micro-scale mechanism of high liquid limit clay treated by recycled construction and demolition wastes (CDW) aggregates
Ma, Q.; et al.
Vol. 332, Article No. 127367, May 2022

2022/126
Mechanical behaviour of multi-panel cross laminated timber shear-walls with stiff connectors
Polastri, A.; Casagrande, D.
Vol. 332, Article No. 127275, May 2022

2022/127
Numerical modelling of steel fibers pull-out from cementitious matrixes
Isla, F.; Argañaraz, P.; Luccioni, B.
Vol. 332, Article No. 127373, May 2022

2022/128
Cross-scale study on the influence of moisture-temperature coupling conditions on adhesive properties of rubberized asphalt and steel slag
Zhang, L.; et al.
Vol. 332, Article No. 127401, May 2022

2022/129
Effect of SBR and XSBRL on water demand, mechanical strength and microstructure of cement paste
Li, X.; et al.
Vol. 332, Article No. 127309, May 2022

2022/130
Effect of curing methods during a long time gap between two printing sessions on the interlayer bonding of 3D printed cementitious materials
Chen, Y.; et al.
Vol. 332, Article No. 127394, May 2022

2022/131
Mechanical behavior, failure pattern and damage evolution of fiber-reinforced cemented sulfur tailings backfill under uniaxial loading
Yin, S.; et al.
Vol. 332, Article No. 127248, May 2022

2022/132
Experimental out-of-plane damage limits of historical stone masonry walls
Misir, I. S.; et al.
Vol. 333, Article No. 127098, May 2022

2022/133
Hydration kinetics and phase evolution of Portland cement composites containing sodium-montmorillonite functionalized with a Non-Ionic surfactant
Luo, D.; Wei, J.
Vol. 333, Article No. 127386, May 2022

2022/134
Evaluation of the phase composition, microstructure, mechanical performance, and resistance to acid attack of blended cement paste composed of binary trass-cement system
Ghasemi, A.; et al.
Vol. 333, Article No. 127356, May 2022

2022/135
A new insight into utilization of red mud in poly(vinyl chloride) composites via surface modification and toughening modulation to attain performance optimization
Ding, C.; et al.
Vol. 333, Article No. 127340, May 2022

2022/136
The slippage effect of concrete gas permeability and the influence of its microstructure
Zhang, J.; et al.
Vol. 333, Article No. 127384, May 2022

2022/137
Development of cost-effective repair system for locally damaged long-distance oil pipelines
Fan, T.; et al.
Vol. 333, Article No. 127342, May 2022

2022/138
Mechanical behavior and recoverable properties of CFRP shape memory alloy composite under different prestrains
Xue, Y. J.; et al.
Vol. 333, Article No. 127186, May 2022

2022/139
Mechanical properties and compressive constitutive relation of solid waste-based concrete activated by soda residue-carbide slag
Guo, W.; et al.
Vol. 333, Article No. 127352, May 2022

2022/140
Molecular dynamics simulation on cohesion and adhesion properties of the emulsified cold recycled mixtures
Wu, M.; et al.
Vol. 333, Article No. 127403, May 2022

2022/141
Shrinkage and sorptivity of mortars with thermoactivated recycled cement
Carriço, A.; et al.
Vol. 333, Article No. 127392, May 2022

2022/142
An innovative location-dependent stochastic model for prediction steel bars area under chloride ion attack in the presence of transverse rebars
Reshvanlou, B. A.; et al.
Vol. 333, Article No. 127390, May 2022

2022/143
Effects of the fly ash and water glass on the mechanical properties and water stability of the high ductile magnesium phosphate cement-based composite
Feng, H.; et al.
Vol. 333, Article No. 127395, May 2022

2022/144
Prediction of the frost resistance of high-performance concrete based on RF-REF: A hybrid prediction approach
Wu, X.; et al.
Vol. 333, Article No. 127132, May 2022

2022/145
Potential use of matakaolin as a partial replacement of preformulated lime binder to improve durability of hemp concrete under cyclic wetting/drying aging
Zerrouki, R.; et al.
Vol. 333, Article No. 127389, May 2022

2022/146
Evolution characteristics of the surface texture of the wearing course on asphalt pavement based on accelerated pavement polishing
Zhu, S.; et al.
Vol. 333, Article No. 127266, May 2022

2022/147
Modeling and experimental study on chloride migration of interfacial transition zone based on its pore structure
Li, C.; et al.
Vol. 333, Article No. 127383, May 2022

2022/148
Study on macroscopic properties and microstructure of thermosetting polyurethane asphalt binder (PAB) based on curing kinetics
Cong, P.; et al.
Vol. 333, Article No. 127347, May 2022

2022/149
Effect of fine sand powder on the rheological properties of one-part alkali-activated slag semi-flexible pavement grouting materials
Zhang, S.; et al.
Vol. 333, Article No. 127328, May 2022

2022/150
Insight into the local C-S-H structure and its evolution mechanism controlled by curing regime and Ca/Si ratio
Wang, Z.; et al.
Vol. 333, Article No. 127388, May 2022

2022/151
Micro and/or Nano-Silica modified moderate and high strength concrete: Rheology and synergistic effects on strength, elastic & inelastic behavior and microstructure
Nuri Turkmenoglu, H.; et al.
Vol. 333, Article No. 127404, May 2022

2022/152
Incorporation of bioleached sulfidic mine tailings in one-part alkali-activated blast furnace slag mortar
Niu, H.; et al.
Vol. 333, Article No. 127195, May 2022

2022/153
Experimental research on mechanical and impact properties of lightweight aggregate fiber shotcrete
Jiang, P.; et al.
Vol. 333, Article No. 127402, May 2022

2022/154
Mechanical, absorptive and freeze–thaw properties of pervious concrete applying a bimodal aggregate packing model
Wu, F.; et al.
Vol. 333, Article No. 127445, May 2022

2022/155
Optimizing RAP sieving efficiency of linear vibrating sieve using DEM simulation
Yang, J.; et al.
Vol. 333, Article No. 127442, May 2022

2022/156
Evaluation of the piezoelectric and mechanical behaviors of asphalt pavements embedded with a piezoelectric energy harvester based on multiscale finite element simulations
Du, C.; et al.
Vol. 333, Article No. 127438, May 2022

2022/157
Experimental research on novel RPC-steel composite connections for prefabricated glubam-concrete composite beams
Shan, B.; et al.
Vol. 333, Article No. 127397, May 2022

2022/158
Study on the bonding properties of the interface between ECC and thermal insulation materials under freeze-thaw environment
Shiping, Y.; et al.
Vol. 333, Article No. 127399, May 2022

2022/159
Drying shrinkage characteristics and mechanism primary exploration of MgO-slag mortars
Ma, H.; et al.
Vol. 333, Article No. 127416, May 2022

2022/160
Embedment strength of smooth nails in timber construction – Characteristic and mean values
Iwuoha, S. E.; Seim, W.
Vol. 333, Article No. 127432, May 2022

2022/161
Study on flexural properties of 3D printed lattice-reinforced concrete structures using acoustic emission and digital image correlation

Liu, J.; et al.
Vol. 333, Article No. 127418, May 2022

2022/162
Structural analysis and parametric study ballasted track in sandy regions
Xiao, H.; et al.
Vol. 333, Article No. 127439, May 2022

2022/163
Improving the accuracy of pavement structural quality assessment by correcting numerical hypothetical model of modulus Back-Calculation through GPR
Zhao, W.; et al.
Vol. 333, Article No. 127422, May 2022

2022/164
Internal interfacial interaction analysis of geopolymer-recycled aggregate pervious concrete based on a infiltration model
Xu, F.; et al.
Vol. 333, Article No. 127417, May 2022

2022/165
Reaction kinetics, microstructure and phase evolution of alkali-activated Si-Mn slag during early age
Su, Z.; et al.
Vol. 333, Article No. 127437, May 2022

2022/166
Belite-calcium sulphoaluminate cement prepared by EMR and BS: Hydration characteristics and microstructure evolution behavior
He, W.; et al.
Vol. 333, Article No. 127415, May 2022

2022/167
Confined vs. unreinforced masonry: Construction and shaking table tests of two-storey buildings
Gioffrè, M.; et al.
Vol. 333, Article No. 126961, May 2022

2022/168
Effects of eco powders from solid waste on freeze-thaw resistance of mortar
Sun, C.; et al.
Vol. 333, Article No. 127405, May 2022

2022/169
Investigation on the erosion mechanism of simulated salt conditions on bitumen
Meng, Y.; et al.
Vol. 334, Article No. 127267, June 2022

2022/170
Effect of temperature on nondestructive measurements for air permeability and water sorptivity of cover concrete
Nguyen, M. H.; et al.
Vol. 334, Article No. 127361, June 2022

2022/171
Early-age hydration heat evolution and kinetics of Portland cement containing nano-silica at different temperatures
Bai, S.; Guan, X.; Li, G.
Vol. 334, Article No. 127363, June 2022

2022/172
Modelling of bond behavior of deformed bar embedded in concrete after heating to high temperatures: A mesoscale study
Jin, L.; et al.
Vol. 334, Article No. 127456, June 2022

2022/173
Thermokinetics of capillary absorption and its application in cement-based materials
Wang, D.; et al.
Vol. 334, Article No. 127446, June 2022

2022/174
Investigation of the flexural behavior of textile reinforced concrete with braiding yarn structure

Kurban, M.; et al.
Vol. 334, Article No. 127434, June 2022

2022/175
Contribution of mineral filler to the fatigue damage behaviour of bituminous mastic
Chaudary, M.; et al.
Vol. 334, Article No. 127120, June 2022

2022/176
Resourceful utilization of quarry tailings in the preparation of non-sintered high-strength lightweight aggregates
Wand, S.; et al.
Vol. 334, Article No. 127444, June 2022

2022/177
Viscosity, mechanical properties and phase-separated morphology of waterborne epoxy asphalt
Ji, J.; et al.
Vol. 334, Article No. 127074, June 2022

2022/178
Properties of β-HPG pastes in the presence of α-HPG prepared from phosphogypsum
Qi, H.; et al.
Vol. 334, Article No. 127414, June 2022

2022/179
A comprehensive evaluation of existing and new model-identification approaches for non-destructive concrete strength assessment
Saleh, E. F.; Tarawneh, A. N.; Katkhuda, H. N.
Vol. 334, Article No. 127447, June 2022

2022/180
A data-driven multi-scale constitutive model of concrete material based on polynomial chaos expansion and stochastic damage model
He, J.; Gao, R.; Tang, Z.
Vol. 334, Article No. 127441, June 2022

2022/181
Experimental study of the shear performance of H-shaped aluminum-timber composite connections
Zhou, Y.; et al.
Vol. 334, Article No. 127421, June 2022

2022/182
Compressive strength and microstructural analysis of recycled coarse aggregate concrete treated with silica fume
Zhu, L.; et al.
Vol. 334, Article No. 127453, June 2022

2022/183
Low-temperature thermal cracking performance of waterborne epoxy asphalt emulsion mastic based on bending beam rheometer (BBR)
Ren, H.; et al.
Vol. 334, Article No. 127461, June 2022

2022/184
Experimental and probabilistic investigation on the durability of geopolymer concrete confined with fiber reinforced polymer
Anvari, M.; Toufigh, V.
Vol. 334, Article No. 127419, June 2022

2022/185
Development of terminal blend rubber and SBS modified asphalt: A case study
Liu, Z.; Wang, Z.
Vol. 334, Article No. 127459, June 2022

2022/186
Sustainability of alternative reinforcement for concrete structures: Life cycle assessment of basalt FRP bars
Pavlović, A.; et al.
Vol. 334, Article No. 127424, June 2022

2022/187
Influence of natural zeolite on fresh properties, compressive strength, flexural strength,

abrasion resistance, Cantabro-loss and microstructure of self-consolidating concrete
Zolghadri, A.; Ahmadi, B.; Taherkhani, H.
Vol. 334, Article No. 127440, June 2022

2022/188
Investigation of the mechanical and shrinkage properties of plastic-rubber compound modified cement mortar with recycled tire steel fiber
Su, P.; et al.
Vol. 334, Article No. 127391, June 2022

2022/189
Research on low-temperature performance of steel slag/polyester fiber permeable asphalt mixture
Zhang, T.; et al.
Vol. 334, Article No. 127214, June 2022

2022/190
Assessment of bonding durability of CLT and glulam made from oak and mixed poplar-oak according to bonding pressure and glue type
Purba, C. Y.; et al.
Vol. 335, Article No. 127345, June 2022

2022/191
Thermodynamic modeling of the influence of temperature on the hydrate phase assemblage in MOC
Han, W.; Chen, H.; Li, X.
Vol. 335, Article No. 127531, June 2022

2022/192
Comparison of different machine learning methods for estimating compressive strength of mortars
Çalışkan, A.; Demirhan, S.; Tekin, R.
Vol. 335, Article No. 127490, June 2022

2022/193
Construction and demolition waste stabilization through a bio-carbonation of reactive magnesia cement for underwater engineering
Wang, D. L.; et al.
Vol. 335, Article No. 127458, June 2022

2022/194
Revealing the co-doping effects of fluorine and copper on the formation and hydration of cement clinker
Da, Y.; et al.
Vol. 335, Article No. 127516, June 2022

2022/195
Effects of concrete materials on the vibration of the adjacent tunnel and surroundings by DEM and experiment
Wu, L.; et al.
Vol. 335, Article No. 127477, June 2022

2022/196
Effects of moulding pressure and w/c induced pore water saturation on the CO2 curing efficiency of dry-mix cement blocks
Tiong, M.; et al.
Vol. 335, Article No. 127509, June 2022

2022/197
Study on the mechanical properties of 3D printing concrete layers and the mechanism of influence of printing parameters
Huang, X.; et al.
Vol. 335, Article No. 127496, June 2022

2022/198
The effect of slag chemistry on the reactivity of synthetic and commercial slags
Zhang, Y.; et al.
Vol. 335, Article No. 127493, June 2022

2022/199
Effect of magnesia expansion agent with different activity on mechanical property, autogenous shrinkage and durability of concrete
Tian, L.; et al.
Vol. 335, Article No. 127506, June 2022

2022/200
Effect of fillers on the mechanical properties and durability of steel slag concrete
Lai, M. H.; et al.
Vol. 335, Article No. 127495, June 2022

2022/201
Yield mechanisms of base shear connections for cross-laminated timber shear walls
Daneshvar, H.; et al.
Vol. 335, Article No. 127498, June 2022

2022/202
Numerical simulation of the stiffness evolution with curing of pavement sections rehabilitated using cold in-place recycling technology
Orosa, P.; et al.
Vol. 335, Article No. 127487, June 2022

2022/203
Experimental investigation of shear strength parameters of ballast encased with geogrid
Esmaeili, M.; Pourrashnoo, A.
Vol. 335, Article No. 127491, June 2022

2022/204
Optimization design and verification of SMA-13 mixture gradation using mortar theory
Xue, J.; et al.
Vol. 335, Article No. 127478, June 2022

2022/205
The internal temperature field of shotcrete in high geothermal tunnel and its effect on microstructures and mechanical properties
Yuan, Q.; et al.
Vol. 335, Article No. 127507, June 2022

2022/206
Evaluation of self-healing in concrete using linear and nonlinear resonance spectroscopy
Kim, R.; et al.
Vol. 335, Article No. 127492, June 2022

2022/207
Anti-fatigue performance of warm-mixed rubber powder modified asphalt mixture based on the DIC technique
Jiang-san, H.; Lan, W.; Xin, L.
Vol. 335, Article No. 127489, June 2022

2022/208
Investigation of failure mechanism of cement-fiber-tailings matrix composites using digital image correlation and acoustic emission
Zhao, K.; et al.
Vol. 335, Article No. 127513, June 2022

2022/209
Variation on the morphology and tensile strength of basalt fiber processed in alkali solutions
Li, M.; et al.
Vol. 335, Article No. 127512, June 2022

2022/210
A novel epoxy-terminated polyethylene modified asphalt with low-viscosity and high storage stability
Li, M.; et al.
Vol. 335, Article No. 127473, June 2022

2022/211
Prediction of moisture resistance of asphalt mastics modified by liquid anti stripping based on support vector regression, artificial neural network and Kernel-based support vector regression methods
Babagoli, R.; Rezaei, M.
Vol. 335, Article No. 127480, June 2022

2022/212
Influence of anode material on the effect of electrophoretic deposition for the repair of rust-cracked reinforced concrete
Wang, Y.; et al.
Vol. 335, Article No. 127466, June 2022

2022/213
Thermal ageing mechanism of a natural rock-modified asphalt binder using Fourier Transform Infrared Spectroscopy analysis
Ma, F.; et al.
Vol. 335, Article No. 127494, June 2022

2022/214
Fatigue life and cracking characterization of engineered cementitious composites (ECC) under flexural cyclic load
Sun, R.; et al.
Vol. 335, Article No. 127465, June 2022

2022/215
Analysis of the trend in evolution of multilevel mechanical properties of solvent-based cold mixed liquid asphalt and mixture
Pei, Z.; et al.
Vol. 335, Article No. 127476, June 2022

2022/216
Characterization of nanoscale cracking at the interface between virgin and aged asphalt binders based on molecular dynamics simulations
Yaphary, Y. L.; et al.
Vol. 335, Article No. 127475, June 2022

2022/217
Mechanical characteristics and analytical model of CLT-concrete composite connections under monotonic loading
Cao, J.; et al.
Vol. 335, Article No. 127472, June 2022

2022/218
Mechanical properties and microstructure of ultra-high-performance concrete with high elastic modulus
Chu, H.; et al.
Vol. 335, Article No. 127385, June 2022

2022/219
Interaction between composition and microstructure of cement paste and polymeric carbon nitride
Yang, Y.; et al.
Vol. 335, Article No. 127464, June 2022

2022/220
Water resistance and mechanical properties of bamboo scrimber composite made from different units of Bambusa chungii as a function of resin content
Rao, F.; et al.
Vol. 335, Article No. 127250, June 2022

2022/221
A new in-situ growth strategy to achieve high performance graphene-based cement material
Yao, Y.; et al.
Vol. 335, Article No. 127451, June 2022

2022/222
Performances of rubber asphalt with middle/high content of waste tire crumb rubber
Zhu, Y.; et al.
Vol. 335, Article No. 127488, June 2022

2022/223
A eco-friendly acid fly ash geopolymer with a higher strength
Pu, S.; et al.
Vol. 335, Article No. 127450, June 2022

2022/224
Experimental study on lauryl alcohol/expanded graphite composite phase change materials for thermal regulation in building
Wu, M.; Liu, C.; Rao, Z.
Vol. 335, Article No. 127400, June 2022

2022/225
Investigating on polymerization process and interaction mechanism of thermosetting polyurethane modified asphalt

Yang, F.; et al.
Vol. 335, Article No. 127261, June 2022

2022/226
Economic and environmental analysis of crumb rubber modified asphalt
Riekstins, A.; Haritonovs, V.; Straupe, V.
Vol. 335, Article No. 127468, June 2022

2022/227
Mechanical properties and deformation mechanism of stratified cemented tailings backfill under unconfined compression
Chen, S.; et al.
Vol. 335, Article No. 127205, June 2022

2022/228
Investigation of a suitable porous stone for the restoration work on the Acropolis circuit wall
Ksinopoulou, E.; Aggelakopoulou, E.; Eleftheriou, V.
Vol. 335, Article No. 127522, June 2022

2022/229
Experimental investigation of temperature gradients in a three-cell concrete box-girder
Feng, Z.; Jinyi, L.; Lei, G.
Vol. 335, Article No. 127413, June 2022

2022/230
Grid nanoindentation on calcium sulfoaluminate (CSA)-Kaolinite pastes
Zakira, U.; et al.
Vol. 335, Article No. 127523, June 2022

2022/231
Hygrothermal, mechanical and durability assessment of vegetable concrete mixes made with Alfa fibers for structural and thermal insulating applications
Charai, M.; et al.
Vol. 335, Article No. 127518, June 2022

2022/232
Performance buildup of concrete cured under low-temperatures: Use of a new nanocomposite accelerator and its application
Zhang, L.; et al.
Vol. 335, Article No. 127529, June 2022

2022/233
Influence of non-linear soil properties on railway critical speed
Fernández-Ruiz, J.; et al.
Vol. 335, Article No. 127485, June 2022

2022/234
Improving workability and mechanical properties of one-part waste brick power based-binders with superplasticizers
Cheng, Y.; et al.
Vol. 335, Article No. 127535, June 2022

2022/235
Hydration mechanisms and mechanical properties of pumice substituted cementitious binder
Pınarcı, İ.; Kocak, Y.
Vol. 335, Article No. 127528, June 2022

2022/236
Innovative use of thermally treated cement-asbestos in the production of foaming materials: Effect of composition, foaming agent, temperature and reaction time
Ligabue, M. L.; et al.
Vol. 335, Article No. 127517, June 2022

2022/237
The quantitative assessment of clogging and cleaning effects on the permeability of pervious concrete
Wang, X.; et al.
Vol. 335, Article No. 127455, June 2022

2022/238
The effect of using recycled PET aggregates on mechanical and durability properties of 3D printed mortar
Skibicki, S.; et al.
Vol. 335, Article No. 127443, June 2022

2022/239
Influence of sustained compressive load on the carbonation of concrete containing blast furnace slag
Liu, Z.; et al.
Vol. 335, Article No. 127457, June 2022

2022/240
Study of dynamic half-cell potential signal of rock bolt under stray current interference based on probabilistic-based method
Wang, C.; et al.
Vol. 335, Article No. 127481, June 2022

2022/241
Self-heating alkali activated materials: Microstructure and its effect on electrical, thermal and mechanical properties
Fiala, L.; et al.
Vol. 335, Article No. 127527, June 2022

2022/242
Influence of aggressive exposure on the degradation of nano-silica admixed cementitious mortar integrated with phase change materials
Snehal, K.; Das, B. B.; Barbhuiya, S.
Vol. 335, Article No. 127467, June 2022

2022/243
Theoretical and experimental study on vibration reduction and frequency tuning of a new damped-sleeper track
He, Z.; et al.
Vol. 336, Article No. 127420, June 2022

2022/244
Early-age hydration and shrinkage of cement paste with coir fibers as studied by Nuclear Magnetic Resonance
Zhang, X.; et al.
Vol. 336, Article No. 127460, June 2022

2022/245
Performance of different binders doped Portland Cement-based mortars using volcanic slag, petroleum coke and EPS foam aggregates
Aygörmez, Y.
Vol. 336, Article No. 127538, June 2022

2022/246
Reactivity and mechanical performance of geopolymer binders from metakaolin/meta-halloysite blends
Kaze, C. R.; et al.
Vol. 336, Article No. 127546, June 2022

2022/247
Investigating dynamic fracture in marble-mortar interface under impact loading
Qiu, H.; et al.
Vol. 336, Article No. 127548, June 2022

2022/248
Stabilization nature and unified strength characterization for cement-based stabilized soils
Liu, L.; et al.
Vol. 336, Article No. 127544, June 2022

2022/249
Monitoring of railway structures with bituminous and granular sub-layers: Assessment after four years of use
Blanc, J.; et al.
Vol. 336, Article No. 127515, June 2022

2022/250
Confined compressive behaviors of high-performance fiber-reinforced concrete and conventional concrete with size effect
Nguyen, D. L.; et al.
Vol. 336, Article No. 127382, June 2022

2022/251
Research on the constitutive relationship of concrete under uniaxial compression in freeze–thaw environment
Gong, X.; et al.
Vol. 336, Article No. 127543, June 2022

2022/252
Three-dimensional corrosion propagation in steel rebars of RC columns with early-age cracks
Vishwanath, B. S.; Banerjee, S.
Vol. 336, Article No. 127335, June 2022

2022/253
Influence of sea salt on the interfacial adhesion of bitumen–aggregate systems by molecular dynamics simulation
Long, Z.; et al.
Vol. 336, Article No. 127471, June 2022

2022/254
Proposed specific heat capacity model for a concrete wall containing phase change material (PCM) under field experiment conditions
Song, H.; et al.
Vol. 336, Article No. 127381, June 2022

2022/255
Effect of rock shear keys on the shear performance of cold joints in rock-filled concrete structures: Experimental and numerical investigation
Zhou, H.; et al.
Vol. 336, Article No. 127315, June 2022

2022/256
Creep of concrete during Alkali-Aggregates Reaction
Lacombe, C.; et al.
Vol. 336, Article No. 127355, June 2022

2022/257
Strain-sensing smart bricks under dynamic environmental conditions: Experimental investigation and new modeling
Meoni, A.; et al.
Vol. 336, Article No. 127375, June 2022

2022/258
Bonding performance of the grooved interface between ultrahigh performance concrete and normal concrete
Tian, J.; et al.
Vol. 336, Article No. 127525, June 2022

2022/259
Synergistic effects of modified sheep wool fibers on impact resistance and strength properties of concrete composites
Alyousef, R.; et al.
Vol. 336, Article No. 127550, June 2022

2022/260
Sensitivity of the strength and toughness of concrete to the properties of the interfacial transition zone
Torrence, C. E.; et al.
Vol. 336, Article No. 126875, June 2022

2022/261
Performance cement-based composite obtained by in-situ growth of organic–inorganic frameworks during the cement hydration
Yin, B.; et al.
Vol. 336, Article No. 127533, June 2022

2022/262
New floating slab track isolator for vibration reduction using particle damping vibration absorption and bandgap vibration resistance
Zhao, C.; et al.
Vol. 336, Article No. 127561, June 2022

2022/263
Comparative modal analysis of B70 and LCR-6 type railway sleepers after repeated impact loads
Çeçen, F.; et al.
Vol. 336, Article No. 127563, June 2022

2022/264
Numerical analysis of train-track-subgrade dynamic performance with crumb rubber in ballast layer
Guo, Y.; et al.
Vol. 336, Article No. 127559, June 2022

2022/265
Promotion effects of gypsum on carbonation of aluminates in medium Al ladle furnace refining slag
Wang, X.; et al.
Vol. 336, Article No. 127567, June 2022

2022/266
Carbonation-hardening properties and ITZ microstructure of low-calcium CO2 sequestration binder mortar
Chang, X.; et al.
Vol. 336, Article No. 127589, June 2022

2022/267
Research on the dynamic impact performance of polyurethane cement-based composite
Lei, Z.; et al.
Vol. 336, Article No. 127574, June 2022

2022/268
Durability degradation of tunnel-lining-shotcrete exposed to nitric acid: Neutralization and nitrate ion migration
Wang, J.; et al.
Vol. 336, Article No. 127554, June 2022

2022/269
Anchorage performance of a modified cable anchor subjected to different joint opening conditions
Chen, J.; et al.
Vol. 336, Article No. 127558, June 2022

2022/270
Design and construction of a new Mechanised Cement Bound Macadam (MCBM)
Blerk, P. G. L. V.; Costello, S. B.; Henning, T. F. P.
Vol. 336, Article No. 127542, June 2022

2022/271
Predicting compressive strength of alkali-activated systems based on the network topology and phase assemblages using tree-structure computing algorithms
Bhat, R.; et al.
Vol. 336, Article No. 127557, June 2022

2022/272
Using 3D printed formworks for the creation of steel fibre reinforced concrete-plastic columns
Katzer, J.; Skoratko, A.
Vol. 337, Article No. 127586, June 2022

2022/273
Adhesion behavior and deposition morphology of cement grout flowing through granular materials
Wang, W.; et al.
Vol. 337, Article No. 127547, June 2022

2022/274
Corrosion monitoring for prestressed concrete cylinder pipe spigot with combined use of Tafel

extrapolation and surface acoustic wave methods
Wang, X.; et al.
Vol. 337, Article No. 127572, June 2022

2022/275
Influence of nano-silica modified rubber mortar and EVA modified porous asphalt on the performance improvement of modified semi-flexible pavement
Davoodi, A.; et al.
Vol. 337, Article No. 127573, June 2022

2022/276
Structural damage-causing concrete cracking detection based on a deep-learning method
Han, X.; et al.
Vol. 337, Article No. 127562, June 2022

2022/277
Development of 3D printable self-sensing cementitious composites
Wang, L.; Aslani, F.; Mukherjee, A.
Vol. 337, Article No. 127601, June 2022

2022/278
Influence of swelling-degradation degree on rheological properties, thermal pyrolysis kinetics, and emission components of waste crumb rubber modified bitumen
Ren, S.; et al.
Vol. 337, Article No. 127555, June 2022

2022/279
Effect of laboratory oxidative aging on dynamic shear rheometer measures of asphalt binder fatigue cracking resistance
Yang, K.; et al.
Vol. 337, Article No. 127566, June 2022

2022/280
Use of recycled concrete aggregates as carriers for self-healing of concrete cracks by bacteria with high urease activity
Wang, X.; et al.
Vol. 337, Article No. 127581, June 2022

2022/281
Properties of water-repellent concrete mortar containing superhydrophobic oyster shell powder
Song, Q.; et al.
Vol. 337, Article No. 127423, June 2022

2022/282
Mechanical behavior of non-persistent joints with different geometric configurations and roughness in solid rock and concrete material
Meng, F.; et al.
Vol. 337, Article No. 127564, June 2022

2022/283
Influence of serpentinite aggregate on the microstructure and durability of radiation shielding concrete
Dąbrowski, M.; et al.
Vol. 337, Article No. 127536, June 2022

2022/284
Mesoscale analysis of concrete under axial compression
Chen, P.; et al.
Vol. 337, Article No. 127580, June 2022

2022/285
Unveiling the cooperation effects of fluorine and copper on tricalcium silicate (C3S) during cement kiln co-processing hazardous wastes containing Cu
Da, Y.; He, T.; Shi, C.
Vol. 337, Article No. 127612, June 2022

2022/286
Production of green bricks from low-reactive copper mine tailings: Durability and environmental aspects
Nikvar-Hassani, A.; Hodges, R.; Zhang, L.
Vol. 337, Article No. 127571, June 2022

2022/287
Influence of pandemic waste face mask on rheological, physical and chemical properties of bitumen
Yalcin, E.; et al.
Vol. 337, Article No. 127576, June 2022

2022/288
A new predictive model for FRCM-confined columns: A reflection on the composite behavior at peak stress
Ameli, Z.; et al.
Vol. 337, Article No. 127534, June 2022

2022/289
The Properties of Cement Paste Incorporating Multi Wall Carbon Nanotube Solution Prepared through Bead Mill and High-Pressure Homogenizer Process with Polycarboxylate Ester
Kim, J. H.; Park, S. H.; Chung, C. W.
Vol. 337, Article No. 127598, June 2022

2022/290
Effects of spatial variability and correlation in stochastic discontinuum analysis of unreinforced masonry walls
Gonen, S.; et al.
Vol. 337, Article No. 127511, June 2022

2022/291
Monitoring and characterization of the polymer-filled pores in sand using nuclear magnetic resonance during air-drying
Wang, Y.; et al.
Vol. 337, Article No. 127568, June 2022

2022/292
Life cycle assessment and mechanical properties of high strength steel fiber reinforced concrete containing waste PET bottle
Nikbin, I. M.; et al.
Vol. 337, Article No. 127553, June 2022

2022/293
Optimization of foam concrete characteristics using response surface methodology and artificial neural networks
Kursuncu, B.; et al.
Vol. 337, Article No. 127575, June 2022

2022/294
The influence of using wet cellulose poultice on nanolime consolidation treatments applied on a limestone
Pozo-Antonio, J. S.; Otero, J.; González, N.
Vol. 337, Article No. 127615, June 2022

2022/295
The role of multi-walled carbon nanotubes for improving C-S-H creep property: An insight from atomic force microscope and nuclear magnetic resonance
Li, H.; et al.
Vol. 337, Article No. 127463, June 2022

2022/296
High density concrete incorporating grit scale aggregates for 4th generation nuclear power plants
Khan, M. N. A.; Yaqub, M.; Malik, A. H.
Vol. 337, Article No. 127578, June 2022

2022/297
Recycling waste disposable medical masks in improving the performance of asphalt and asphalt mixtures
Zhao, Z.; et al.
Vol. 337, Article No. 127621, June 2022

2022/298
Prediction of crushed numbers and sizes of ballast particles after breakage using machine learning techniques
Aela, P.; et al.
Vol. 337, Article No. 127469, June 2022

2022/299
Predicting airborne chloride deposition in marine bridge structures using an artificial neural network model
Jeon, D.; et al.
Vol. 337, Article No. 127623, June 2022

2022/300
Investigation on the concrete strength performance of underlying tunnel structure subjected to train-induced dynamic loads at an early age
Zheng, Y.; et al.
Vol. 337, Article No. 127622, June 2022

2022/301
Shrinkage characteristics of calcium sulphoaluminate cement concrete
Ke, G.; Zhang, J.; Liu, Y.
Vol. 337, Article No. 127627, June 2022

2022/302
Experimental investigation and numerical simulation for chloride diffusivity of cement paste with elliptical cement particles
Zhang, J.; et al.
Vol. 337, Article No. 127616, June 2022

2022/303
Development of rail pads from recycled polymers for ballasted railway tracks
Castillo-Mingorance, J. M.; et al.
Vol. 337, Article No. 127479, June 2022

2022/304
Preparation and properties of foamed cement for lightweight thermal insulation with Ti-extraction blast furnace slag and sulfoaluminate cement by chemical foaming
Li, L.; et al.
Vol. 337, Article No. 127634, June 2022

2022/305
Innovative modeling framework of chloride resistance of recycled aggregate concrete using ensemble-machine-learning methods
Liu, K. H.; et al.
Vol. 337, Article No. 127613, June 2022

2022/306
A novel integrated approach of augmented grey wolf optimizer and ANN for estimating axial load carrying-capacity of concrete-filled steel tube columns
Bardhan, A.; et al.
Vol. 337, Article No. 127454, June 2022

2022/307
Experimental study on the free expansion deformation of concrete during the cooling process after being heated to high temperature
Li, Q.; et al.
Vol. 337, Article No. 127617, June 2022

2022/308
3D printing of cement-based materials with adapted buildability
Moeini, M. A.; Hosseinpoor, M.; Yahia, A.
Vol. 337, Article No. 127614, June 2022

Engineering Structures
2022/309
Curvature response of bridge pier subjected to earthquake action in a saline soil environment
Deng, Y.; et al.
Vol. 258, Article No. 114106, May 2022

2022/310
Zig-zag theory for concrete beams with corrugated steel webs
Zhang, Z. C.; et al.
Vol. 258, Article No. 114100, May 2022

2022/311
Cyclic behavior of bridge columns with partially unbonded seven-wire steel strands to increase post-yield stiffness
Ou, Y. C.; Wu, J. W.; Pratiwi, A. Y.
Vol. 258, Article No. 114112, May 2022

2022/312
Elastic compressive buckling resistance for back-to-back double angle assemblies
Alenezi, A. M.; Mohareb, M.
Vol. 258, Article No. 114120, May 2022

2022/313
Experimental and FE study on strengthened steel beam-column joints for progressive collapse robustness under column-loss event
Alrubaidi, M.; et al.
Vol. 258, Article No. 114103, May 2022

2022/314
Flexural behavior RC beams strengthened and repaired with SRP composite
Sneed, L. H.; et al.
Vol. 258, Article No. 114084, May 2022

2022/315
Failure mode-based calculation method for bending bearing capacities of normal cross-sections of corroded reinforced concrete beams
Jiang, C.; et al.
Vol. 258, Article No. 114113, May 2022

2022/316
Effect of member grouping and pool size of discrete cross-sections on the optimal design of a large-scale 3D steel frame
Turay, B. M.; Fernández-Cabán, P. L.; Thomson, K. J.
Vol. 258, Article No. 114098, May 2022

2022/317
Seismic performance evaluation of eccentrically braced frames with long links using FEMA P695 methodology
Ün, E. M.; Al-Janabi, M. A. Q.; Topkaya, C.
Vol. 258, Article No. 114104, May 2022

2022/318
New predictive equations for LDB strength assessment of steel–concrete composite beams
Hosseinpour, M.; et al.
Vol. 258, Article No. 114121, May 2022

2022/319
Mechanical behavior of steel transmission tower legs reinforced with innovative clamp under eccentric compression
Liang, G.; et al.
Vol. 258, Article No. 114101, May 2022

2022/320
Blind comparison of saturation ratio profiles on large RC structures by means of NDT and SFE—Application to the VeRCoRs mock-up
Gupta, R.; et al.
Vol. 258, Article No. 114057, May 2022

2022/321
In-operation performance evaluation of damped light poles using fatigue life estimations
Desjardins, S.; Poitras, G.
Vol. 258, Article No. 114081, May 2022

2022/322
Numerical modeling of the fire behavior of reinforced concrete tunnel slabs during heating and cooling
Hua, N.; Khorasani, N. E.; Tessari, A.
Vol. 258, Article No. 114135, May 2022

2022/323
Application of an analytical method for the design for robustness of RC flat slab buildings
Martinelli, P.; et al.

Vol. 258, Article No. 114117, May 2022

2022/324
Benchmark tests on high strength steel frames
Yun, X.; et al.
Vol. 258, Article No. 114108, May 2022

2022/325
Machine learning-based wind pressure prediction of low-rise non-isolated buildings
Weng, Y.; Paal, S. G.
Vol. 258, Article No. 114148, May 2022

2022/326
Strength reduction design method for reinforced concrete structures: Generalization
Abra, O.; Ben Ftima, M.
Vol. 258, Article No. 114134, May 2022

2022/327
Flexural strength recovery of RC one-way slabs having cut-outs using NSM-SHCC plates
Khalil, A. E. A.; et al.
Vol. 258, Article No. 114149, May 2022

2022/328
The design of a structural Hyper-resisting element for Life Threatening Earthquake risk (SHELTER) for building collapse scenarios: The life-saving capsule
Gurrreiro, J.; et al.
Vol. 258, Article No. 114151, May 2022

2022/329
Topology optimization of proportionally damped structures under harmonic excitations: Analysis of velocity and acceleration responses
Zhao, X.; et al.
Vol. 258, Article No. 114140, May 2022

2022/330
Numerical issues on brittle shear failure of pier-wall continuous vertical joints in URM dutch buildings
Fusco, D.; et al.
Vol. 258, Article No. 114078, May 2022

2022/331
New approaches for floor vibrations of steel–polymer–steel sandwich floor systems
Park, M. J.; Yoon, S. W.; Ju, Y. K.
Vol. 258, Article No. 114141, May 2022

2022/332
Simplified mechanical models for the seismic collapse performance prediction of unreinforced masonry structures
Yu, L. L.; Dong, Z. Q.; Li, G.
Vol. 258, Article No. 114131, May 2022

2022/333
Numerical and full-scale test case studies on post-elastic performance of transmission towers
Li, J. X.; Zhang, X. H.; McClure, G.
Vol. 259, Article No. 114133, May 2022

2022/334
Seismic response of regular multi-span bridges having buckling-restrained braces in their longitudinal direction
Carrion-Cabrera, H.; Bruneau, M.
Vol. 259, Article No. 114127, May 2022

2022/335
Symmetric and asymmetric thermo-induced buckling and postbuckling of rotating GPLRC annular plates rested on elastic foundation
Yang, Y.; et al.
Vol. 259, Article No. 114110, May 2022

2022/336
Damage detection for constituents of track-bridge systems from driving component of vehicle-rail contact response
Yang, Y. B.; et al.
Vol. 259, Article No. 114143, May 2022

2022/337
Experimental study on seismic behavior of welded H-section stainless steel beam-columns
Chen, Y.; et al.
Vol. 259, Article No. 114105, May 2022

2022/338
Innovative prefabricated lightweight slab system of high structural performance
Barros, J. A. O.; et al.
Vol. 259, Article No. 114146, May 2022

2022/339
A theory-based simplified trilinear model for characterisation of the out-of-plane behaviour of URM walls
Navas-Sánchez, L.; Bravo, J. C.
Vol. 259, Article No. 114058, May 2022

2022/340
Re-evaluation of shear contribution of CFRP and GFRP sheets in concrete beams post-tensioned with unbonded tendons
Vo-Le, D.; et al.
Vol. 259, Article No. 114173, May 2022

2022/341
Free vibration of FGM Mindlin plates submerged in fluid
Li, H. C.; et al.
Vol. 259, Article No. 114144, May 2022

2022/342
Deep learning-based autonomous damage-sensitive feature extraction for impedance-based prestress monitoring
Nguyen, T. T.; et al.
Vol. 259, Article No. 114172, May 2022

2022/343
Cyclic-shear behavior of square thin-walled concrete-filled steel tubular columns with diagonal ribs
Zhou, Z.; Gan, D.; Zhou, X.
Vol. 259, Article No. 114177, May 2022

2022/344
An improved model for the time-dependent material response of wood under mechanical loading and varying humidity conditions
Yu, T.; Khaloian, A.; van de Kuilen, J. W.
Vol. 259, Article No. 114116, May 2022

2022/345
Coupled CFD-FE analysis of a long-span truss beam exposed to spreading fires
Janardhan, R. K.; et al.
Vol. 259, Article No. 114150, May 2022

2022/346
Analysis and optimal control of smart damping for porous functionally graded magneto-electro-elastic plate using smoothed FEM and metaheuristic algorithm
Thoi, T. N.; et al.
Vol. 259, Article No. 114062, May 2022

2022/347
Modelling rotational friction damping devices using the Non-Smooth Dynamics method
Namorado, B.; Pinto da Costa, A.; Simões, F. M. F.
Vol. 259, Article No. 114118, May 2022

2022/348
Peak wind pressures on roof claddings of regular railway stations
Chen, B.; et al.
Vol. 259, Article No. 114178, May 2022

2022/349
Automated identification of compressive stress and damage in concrete specimen using convolutional neural network learned electromechanical admittance
Ai, D.; et al.
Vol. 259, Article No. 114176, May 2022

2022/350
Seismic performance of semi-precast composite columns with bolted end-plate connections to footing
Kim, C. S.; et al.
Vol. 259, Article No. 114174, May 2022

2022/351
Optimization of post-tensioned concrete slabs for minimum cost
Zelickman, Y.; Amir, O.
Vol. 259, Article No. 114132, May 2022

2022/352
Experimental study on the structural performance of full-scale tyre wall for residential housing applications
Xu, Y.; et al.
Vol. 259, Article No. 114181, May 2022

2022/353
Testing, numerical modelling and design of Q690 high strength steel welded T-section stub columns
Liu, J. Z.; et al.
Vol. 259, Article No. 114142, May 2022

2022/354
A computationally efficient framework for the simulation of the nonlinear seismic performance of infilled RC frame buildings
Bose, S.; Stavridis, A.
Vol. 259, Article No. 114039, May 2022

2022/355
Parameter identification of ductile timber beam-to-steel column connections: Procedure and assessment
Liu, J.; Yang, H.
Vol. 259, Article No. 114179, May 2022

2022/356
Cyclic performance of RC bridge piers retrofitted with UHPC jackets: Experimental investigation
Yuan, W.; et al.
Vol. 259, Article No. 114139, May 2022

2022/357
Experimental study and analytical evaluation on seismic performance of CECFST moment resisting frame with bolted connections
Guo, L.; et al.
Vol. 259, Article No. 114074, May 2022

2022/358
Flexural behaviour of 7A04-T6 high-strength aluminium alloy SHS and RHS beams under moment gradient
Li, B.; et al.
Vol. 259, Article No. 114138, May 2022

2022/359
Reliability evaluation of twin steel box girder bridges using a simplified method
Abedin, M.; et al.
Vol. 259, Article No. 114122, May 2022

2022/360
Investigation of strengthened low slenderness RC column by using textile reinforced mortar strip under axial load
Mercimek, Ö.; et al.
Vol. 259, Article No. 114191, May 2022

2022/361
Power-actuated fasteners in single shear-An experimental investigation and proposed design rules
Milewska, A.; et al.
Vol. 259, Article No. 114124, May 2022

2022/362
Large displacement analysis of stiffened plates with parallel ribs under lateral pressure using FE modeling with shell elements
Rezaiefar, A.; Galal, K.
Vol. 259, Article No. 114125, May 2022

2022/363
Proportional flexibility-based damage detection for buildings in unknown mass scenarios: The case of severely truncated modal spaces
Bernagozzi, G.; et al.
Vol. 259, Article No. 114145, May 2022

2022/364
A computer vision-based method for bridge model updating using displacement influence lines
Martini, A.; et al.
Vol. 259, Article No. 114129, May 2022

2022/365
Effect of steel fibers on the ultimate flexural behavior of dapped-end connections
Mihaylov, B.; Rajapakse, C.; Berger, P. H.
Vol. 259, Article No. 114147, May 2022

2022/366
Least Angle Regression for early-stage identification of earthquake-induced damage in a monumental masonry palace
Palazzo dei Consoli García-Macías, E.; Ubertini, F.
Vol. 259, Article No. 114119, May 2022

2022/367
Machine learning-based sensitivity of steel frames with highly imbalanced and high-dimensional data
Koh, H.; Blum, H. B.
Vol. 259, Article No. 114126, May 2022

2022/368
Long-term creep behavior of NC filled UHPC tube composite column
Zhang, Y.; et al.
Vol. 259, Article No. 114214, May 2022

2022/369
Experimental analysis on circular concrete-filled steel tubular beam-columns under unequal load eccentricities
Albero, V.; et al.
Vol. 259, Article No. 114206, May 2022

2022/370
Finite contact duration modeling of a Vibro-Impact Nonlinear Energy Sink to protect a civil engineering frame structure against seismic events
Lo Feudo, S.; et al.
Vol. 259, Article No. 114137, May 2022

2022/371
Topological design of the octahedron tensegrity family
Fernández-Ruiz, M. A.; Hernández-Montes, E.; Gil-Martín, L. M.
Vol. 259, Article No. 114211, May 2022

2022/372
Hybrid joining of jacket structures for offshore wind turbines – Determination of requirements and adhesive characterisation
Albiez, M.; et al.
Vol. 259, Article No. 114186, May 2022

2022/373
Online frequency and amplitude tracking in structural vibrations under environment using APES spectrum postprocessing and Kalman filtering
Yu, X.; Dan, D.
Vol. 259, Article No. 114175, May 2022

2022/374
Empirical seismic fragility assessment and optimal risk mitigation of building contents
Majdalaweyh, S.; Pang, W.
Vol. 259, Article No. 114183, May 2022

2022/375
Unified method for fully automated modal identification and tracking with consideration of sensor deployment
He, M.; et al.
Vol. 260, Article No. 114223, June 2022

2022/376
Data-based model with EMD and a new model selection criterion for dam health monitoring
Bian, K.; Wu, Z.
Vol. 260, Article No. 114171, June 2022

2022/377
Buckling behavior and design of concentrically loaded T-section aluminum alloy columns
Yuan, L.; Zhang, Q.
Vol. 260, Article No. 114221, June 2022

2022/378
Experimental and numerical investigation of lightweight foamed reinforced concrete deep beams with steel fibers
Manharawy, M. S.; et al.
Vol. 260, Article No. 114202, June 2022

2022/379
Performance of SRC column-RC beam joints under combined axial and cyclic lateral loadings
Gautham, A.; Sahoo, D. R.
Vol. 260, Article No. 114218, June 2022

2022/380
An analytical method to determine the post-cracking flexural stress in pretensioned concrete beams
Bastos, J. C.; Edwards, J. R.; Dersch, M. S.
Vol. 260, Article No. 114188, June 2022

2022/381
Coupling machine learning and stochastic finite element to evaluate heterogeneous concrete infrastructure
Salazar, F.; Hariri-Ardebili, M. A.
Vol. 260, Article No. 114190, June 2022

2022/382
A numerical study of erosion void and corrosion effects on the performance of buried corrugated steel culverts
Nakhostin, E.; Kenny, S.; Sivathayalan, S.
Vol. 260, Article No. 114217, June 2022

2022/383
Tensile behaviour of CFRP-glass adhesively bonded connections: double-lap joint tests and numerical modelling
Rocha, J.; Sena-Cruz, J.; Pereira, E.
Vol. 260, Article No. 114212, June 2022

2022/384
Structural symmetry recognition in planar structures using Convolutional Neural Networks
Zhang, P.; et al.
Vol. 260, Article No. 114227, June 2022

2022/385
Vibration-based Bayesian model updating of an actual steel truss bridge subjected to incremental damage
Zhou, X.; et al.
Vol. 260, Article No. 114226, June 2022

2022/386
Interfacial shear and flexural performances of steel–precast UHPC composite beams: Full-depth slabs with studs vs. demountable slabs with bolts
Fang, Z.; et al.
Vol. 260, Article No. 114230, June 2022

2022/387
Behaviour of unreinforced masonry walls retrofitted by using basalt textile reinforced mortar
Ibrahim, M.; et al.
Vol. 260, Article No. 114201, June 2022

2022/388
Reduced and test-data correlated FE-models of a large timber truss with dowel-type connections aimed for dynamic analyses at serviceability level
Landel, P.; Linderholt, A.
Vol. 260, Article No. 114208, June 2022

2022/389
A serviceability investigation of dowel-type timber connections featuring single softwood dowels
Wilkinson, G.; Augarde, C.
Vol. 260, Article No. 114210, June 2022

2022/390
Initial parameters to estimate the fatigue strength of welded structures using a fracture mechanical model
Skoglund, O.; Leander, J.
Vol. 260, Article No. 114185, June 2022

2022/391
Experimental testing of full-scale fiber reinforced elastomeric isolators (FREIs) in unbounded configuration
Losanno, D.; De Domenico, D.; Madera-Sierra, I. E.
Vol. 260, Article No. 114234, June 2022

2022/392
Development of novel SMA-based D-type self-centering eccentrically braced frames
Chen, Z. P.; et al.
Vol. 260, Article No. 114228, June 2022

2022/393
Axial compressive behavior and modeling of fiber-reinforced polymer-concrete-steel double-skin tubular stub columns with a rectangular outer tube and an elliptical inner tube
Wang, Y.; et al.
Vol. 260, Article No. 114222, June 2022

2022/394
Modeling the shear behavior of deep beams strengthened with FRP sheets
Fathalla, E.; Rajapakse, R. M. C. M.; Mihaylov, B. I.
Vol. 260, Article No. 114232, June 2022

2022/395
Response spectrum model of vehicle dynamic load for the prediction of bridge vibration level due to single vehicle-passage
Wang, H.; Nagayama, T.
Vol. 260, Article No. 114180, June 2022

2022/396
Effect of corrosion on the tensile and fatigue performance of CFRP strand Sheet/Steel double strap joints
Ren, X.; et al.
Vol. 260, Article No. 114240, June 2022

2022/397
Seismic damage and life cycle cost assessment of unanchored brick masonry veneers
Khalili, M. R.; Baghmisheh, A. G.; Estekanchi, H. E.
Vol. 260, Article No. 114187, June 2022

2022/398
Experimental and nonlinear FE simulation-based compressive behavior of stiffened FRP-concrete-steel double-skin tubular columns with square outer and circular inner tubes
Zakir, M.; Sofi, F. A.
Vol. 260, Article No. 114237, June 2022

2022/399
Demands on acceleration-sensitive nonstructural components in special concentrically braced frame and special moment frame buildings
Salari, N.; et al.
Vol. 260, Article No. 114031, June 2022

2022/400
Investigation of shear and flexural failures of dapped-end connections with orthogonal reinforcement
Rajapakse, C.; Degée, H.; Mihaylov, B.
Vol. 260, Article No. 114233, June 2022

2022/401
Equivalent stress-strain model of half grouted sleeve connection under monotonic and repeated loads: Experiment and preliminary application
Zhang, X.; et al.
Vol. 260, Article No. 114247, June 2022

2022/402
Time-domain numerical analysis of single pedestrian random walks on laminated glass slabs in pre- or post-breakage regime
Bedon, C.
Vol. 260, Article No. 114250, June 2022

2022/403
Experimental and numerical study on bent shear panel damper made of BLY160 steel
Zhao, J. Z.; et al.
Vol. 260, Article No. 114229, June 2022

2022/404
Effects of gaps on the rotational performance of traditional straight mortise-tenon joints
Zhang, B.; et al.
Vol. 260, Article No. 114231, June 2022

2022/405
Basin effects on tall bridges in Seattle from M9 Cascadia scenarios
Somala, S. N.; Parla, R.; Mangalathu, S.
Vol. 260, Article No. 114252, June 2022

2022/406
A machine-learning-based model for predicting the effective stiffness of precast concrete columns
Wang, Z.; et al.
Vol. 260, Article No. 114224, June 2022

2022/407
Bond degradation and EMI-based monitoring of CFRP to concrete interfaces exposed to wet-dry cycling
Zhu, M.; et al.
Vol. 260, Article No. 114225, June 2022

2022/408
Fragility functions for highway RC bridge under various flood scenarios
Anisha, A.; et al.
Vol. 260, Article No. 114244, June 2022

2022/409
A model for stud groups subjected to shear and moment
Stanton, J. F.; Calvi, P. M.
Vol. 260, Article No. 114182, June 2022

2022/410
Experimental validation of damaged reinforced concrete beam strengthened by pretensioned prestressed ultra-high-performance concrete layer
Zhang, Y.; et al.
Vol. 260, Article No. 114251, June 2022

2022/411
Analysis of torsionally loaded non-uniform circular piles in multi-layered non-homogeneous elastic soils
Vega-Posada, C. A.; Areiza-Hurtado, M.
Vol. 260, Article No. 114205, June 2022

2022/412
Proposed auxetic cluster designs for lightweight structural beams with improved load bearing capacity
Menon, H. G.; et al.
Vol. 260, Article No. 114241, June 2022

2022/413
Effect of the web hole size on the axial capacity of back-to-back aluminium alloy channel section columns
Fang, Z.; et al.
Vol. 260, Article No. 114238, June 2022

2022/414
Neural-network based wind pressure prediction for low-rise buildings with genetic algorithm and Bayesian optimization
Ding, Z.; Zhang, W.; Zhu, D.
Vol. 260, Article No. 114203, June 2022

2022/415
Active isolation tests of metamaterial-based barriers and foundation
Wang, J.; et al.
Vol. 260, Article No. 114253, June 2022

2022/416
Novel hysteretic damper to improve the distribution of story drifts and energy dissipation along the height of braced frames
Milani, A. S.; Dideli, M.
Vol. 260, Article No. 114264, June 2022

2022/417
Experimental and numerical study on the bending response of a prefabricated composite CLT-steel floor module
Owolabi, D.; Loss, C.
Vol. 260, Article No. 114278, June 2022

2022/418
Cyclic behavior and design methodology of exposed base plates with extended anchor bolts
Torres-Rodas, P.; et al.
Vol. 260, Article No. 114235, June 2022

2022/419
Numerical and experimental investigations on the welding residual stresses and distortions of the short fillet welds in high strength steel plates
Ghafouri, M.; et al.
Vol. 260, Article No. 114269, June 2022

2022/420
Shear capacity of prestressed hollow core slabs in flexible support using computational modelling
Rosa de Souza, J.; de Lima Araújo, D.;
Vol. 260, Article No. 114243, June 2022

2022/421
Prediction of axial compressive capacity of CFRP-confined concrete-filled steel tubular short columns based on XGBoost algorithm
Ma, L.; et al.
Vol. 260, Article No. 114239, June 2022

2022/422
Longitudinal shear performance of lightweight steel-UHPC composite connections based on large-diameter high strength friction-grip bolts
Xu, Q.; et al.
Vol. 260, Article No. 114220, June 2022

2022/423
Seismic behavior of circular CFST columns with different internal constructions
Dong, H.; et al.
Vol. 260, Article No. 114262, June 2022

2022/424
Statically equivalent seismic loads based on two-mode-based approach for single layer reticulated shells
Takiuchi, Y.; et al.
Vol. 260, Article No. 114242, June 2022

2022/425
Effectiveness of buckling restrained braces for upgrading earthquake resistant capacity of single layer grid dome
Kato, S.; et al.
Vol. 261, Article No. 114280, June 2022

2022/426
Buffeting response of a suspension bridge based on the 2D rational function approximation model for self-excited forces
Barni, N.; Øiseth, O. A.; Mannini, C.
Vol. 261, Article No. 114267, June 2022

2022/427
Modeling stiffness of connections and non-structural elements for dynamic response of taller glulam timber frame buildings
Tulebekova, S.; et al.
Vol. 261, Article No. 114209, June 2022

2022/428
Seismic performance of joint between L-shaped CFST column and H-section beam with lower plate and extended flange plate
Liu, X. C.; Wu, X. T.; Chen, X.
Vol. 261, Article No. 114283, June 2022

2022/429
Damage evaluation of a welded beam–column joint with surface imperfections subjected to impact loads
Chen, Y.; et al.
Vol. 261, Article No. 114276, June 2022

2022/430
Assessment by finite element modeling of pipelines with corrosion defects based on River-Bottom Profile model
Cabral, R. M. S.; et al.
Vol. 261, Article No. 114246, June 2022

2022/431
Analysis of the tension chord in the flexural response of concrete elements: Methodology and application to weft-knitted textile reinforcement
Lee, M.; Mata-Falcón, J.; Kaufmann, W.
Vol. 261, Article No. 114270, June 2022

2022/432
Performance-based seismic design and assessment of multi-storey CFS strap-braced frames
Papargyriou, I.; Hajirasouliha, I.
Vol. 261, Article No. 114268, June 2022

2022/433
Bridge deformation prediction based on SHM data using improved VMD and conditional KDE
Xin, J.; et al.
Vol. 261, Article No. 114285, June 2022

2022/434
Flexibility matrix identification using the moving vehicle induced responses for beam type bridge
He, W. Y.; et al.
Vol. 261, Article No. 114277, June 2022

2022/435
Load transfer mechanism of precast concrete piers with demountable connections
Zhou, Q.; Liu, Y.; Li, Y.
Vol. 261, Article No. 114287, June 2022

2022/436
Shear transfer mechanism in reinforced engineered cementitious composite (ECC) beams: Quantification of VS and VC
Gu, D.; et al.
Vol. 261, Article No. 114282, June 2022

2022/437
Experimental and numerical investigations on moment redistribution in reinforced concrete frames subjected to vertical loads
Li, L.; et al.
Vol. 261, Article No. 114289, June 2022

2022/438
Non-linear necking behaviour of S275 to S960 structural steels under monotonic tension
Ho, H. C.; et al.
Vol. 261, Article No. 114263, June 2022

2022/439
Interpretation of simultaneously optimized fuzzy controller and active tuned mass damper parameters under Pulse-type ground motions
Lavassani, S. H. H.; et al.
Vol. 261, Article No. 114286, June 2022

2022/440
Experimental verification of a beam element for thin-walled beams with torsion, distortion, and shear lag
Cambronero-Barrientos, F.; et al.
Vol. 261, Article No. 114249, June 2022

2022/441
Effect of dampers on the seismic performance of masonry walls assessed through fragility and demand hazard curves
Giresini, L.; et al.
Vol. 261, Article No. 114295, June 2022

2022/442
Shear behavior of innovative high performance joints for precast concrete deck panels
Hu, M.; et al.
Vol. 261, Article No. 114307, June 2022

2022/443
Flexural behavior of fire-damaged concrete beams repaired with strain-hardening cementitious composite
Li, X.; et al.
Vol. 261, Article No. 114305, June 2022

2022/444
Accurate thermal-induced structural failure analysis under incompressible conditions
Moreira, C. A.; et al.
Vol. 261, Article No. 114213, June 2022

2022/445
Experimental study on seismic behavior of the self-centering RCS joint with replaceable buckling restrained dampers
Yang, Y.; et al.
Vol. 261, Article No. 114288, June 2022

2022/446
Structural damage identification considering uncertainties based on a Jaya algorithm with a local pattern search strategy and L0.5 sparse regularization
Ding, Z.; Hou, R.; Xiz, Y.
Vol. 261, Article No. 114312, June 2022

2022/447
Multi-objective reliability-based seismic performance design optimization of SMRFs considering various sources of uncertainty
Rastegaran, M.; Aval, S. B. B.; Sangalaki, E.
Vol. 261, Article No. 114219, June 2022

International Journal of Fatigue

2022/448
Fatigue behavior of hybrid multi-bolted-bonded single-lap joints in woven composite plates
Gamdani, F.; Boukhili, R.; Vadean, A.
Vol. 158, Article No. 106738, May 2022

2022/449
Effect of surface nanocrystallization on high-cycle fatigue behavior of Ti–2Al–2.5Zr alloy tube
Chen, G.; et al.
Vol. 158, Article No. 106735, May 2022

2022/450
On the mechanism of fatigue crack initiation in high-angle grain boundaries
Mazánová, V.; Heczko, M.; Polák, J.
Vol. 158, Article No. 106721, May 2022

2022/451
Multiaxial fatigue assessment of welded joints using a principal component-based measure for non-proportionality
Larsen, M. L.; et al.
Vol. 158, Article No. 106731, May 2022

2022/452
Statistical inference of the Equivalent Initial Flaw Size Distribution for an anisotropic material with the Dual Boundary Element Method
Zhuang, M.; et al.
Vol. 158, Article No. 106702, May 2022

2022/453
Gaussian process regression based remaining fatigue life prediction for metallic materials under two-step loading
Gao, J.; et al.
Vol. 158, Article No. 106730, May 2022

2022/454
Comparative study of critical plane fatigue criteria on multiaxial variable amplitude loaded welded test specimens
Bibbo, N. D.; Baumgartner, J.; Arora, V.
Vol. 158, Article No. 106670, May 2022

2022/455
Microstructures and fatigue behaviors of 25CrNi2MoV steel under electropulsing-assisted ultrasonic surface rolling
Duan, C.; et al.
Vol. 158, Article No. 106733, May 2022

2022/456
Prediction of anisotropic LCF behavior for SLM Ti-6Al-4V considering the spatial orientation of defects
Hu, D.; et al.
Vol. 158, Article No. 106734, May 2022

2022/457
Accounting for crack closure effects in out-of-phase TMF crack growth with extended hold times
Loureiro-Homs, J.; et al.
Vol. 158, Article No. 106740, May 2022

2022/458
Microstructure evolution and mechanical properties of martensite stainless steel during repetitive high stress Loading-Unloading with small plastic deformation
Wei, Y.; et al.
Vol. 158, Article No. 106750, May 2022

2022/459
Fatigue crack growth acceleration in S355 steel under a single and periodic underload
Liang, H.; et al.
Vol. 158, Article No. 106744, May 2022

2022/460
Surface rolling deformed severity-dependent fatigue mechanism of Ti-6Al-4V alloy
Ao, N.; et al.
Vol. 158, Article No. 106732, May 2022

2022/461
Fatigue life estimating for chloride attacked RC beams using the S-N curve combined with mesoscale simulation of chloride ingress
Wu, J.; et al.
Vol. 158, Article No. 106751, May 2022

2022/462
Fatigue crack initiation behaviors around defects induced by welding thermal cycle in superalloy IN617B
Li, S.; et al.
Vol. 158, Article No. 106745, May 2022

2022/463
Determination of the fatigue equation for the cement-stabilized cold recycled mixtures with road construction waste materials based on data-driven
Ren, J.; et al.
Vol. 158, Article No. 106765, May 2022

2022/464
Rail rolling contact fatigue formation and evolution with surface defects
Zhang, S. Y.; et al.
Vol. 158, Article No. 106762, May 2022

2022/465
Laboratory accelerated loading test to investigate the fatigue algorithm of the interface debonding of bonded concrete overly of Asphalt
Mu, F.; Vandenbossche, J. M.
Vol. 158, Article No. 106665, May 2022

2022/466
Multiscale modelling strategy for predicting fatigue lives and limits of steels based on a generalised evaluation method of grain boundaries effects
Zhou, H.; et al.
Vol. 158, Article No. 106749, May 2022

2022/467
Rubber fatigue prediction for filled natural rubber under positive and negative R ratios
Luo, R. K.
Vol. 158, Article No. 106769, May 2022

2022/468
Defect-induced cracking and fine granular characteristics in very-high-cycle fatigue of laser powder bed fusion AlSi10Mg alloy
Li, J.; et al.
Vol. 158, Article No. 106770, May 2022

2022/469
A nonlinear constant life diagram model for out-of-plane shear fatigue life prediction of 3D woven composites
Guo, L.; et al.
Vol. 158, Article No. 106746, May 2022

2022/470
Fatigue life prediction considering mean stress effect based on random forests and kernel extreme learning machine
Gan, L.; Wu, H.; Zhong, Z.
Vol. 158, Article No. 106761, May 2022

2022/471
Failure diagrams for subcritical crack growth
Sadananda, K.; Iyyer, N.
Vol. 158, Article No. 106775, May 2022

2022/472
Multiaxial fatigue behaviour and damage mechanisms of P92 steel under various strain amplitudes and strain ratios at high temperature
Gao, N.; et al.
Vol. 158, Article No. 106774, May 2022

2022/473
Effect of voids on fatigue damage propagation in 3D5D braided composites revealed via automated algorithms using X-ray computed tomography
Liu, X.; et al.
Vol. 158, Article No. 106778, May 2022

2022/474
A finite element study on the influence of the hardening behavior on plasticity-induced fatigue crack closure
Reichenbacher, A.; et al.
Vol. 158, Article No. 106768, May 2022

2022/475
Machine learning based very-high-cycle fatigue life prediction of Ti-6Al-4V alloy fabricated by selective laser melting
Li, J.; et al.
Vol. 158, Article No. 106764, May 2022

2022/476
Extreme variation in fatigue: Fatigue life prediction and dependence on build volume

location in laser powder bed fusion of 17-4 stainless steel
Berez, J.; Sheridan, L.; Saldaña, C.
Vol. 158, Article No. 106737, May 2022

2022/477
A combined elastic–plastic framework unifying the various cyclic softening/hardening behaviors for heat resistant steels: Experiment and modeling
Song, K.; et al.
Vol. 158, Article No. 106736, May 2022

2022/478
Influence of normal load frequency on fretting fatigue behaviour by a critical plane-based approach
Vantadori, S.; et al.
Vol. 158, Article No. 106724, May 2022

2022/479
A simple strategy to perform mixed-mode I+II fatigue/fracture characterisation of composite bonded joints
Moreira, R. D. F.; et al.
Vol. 158, Article No. 106723, May 2022

2022/480
Effect of rock bridge length on fracture and damage modelling in granite containing hole and fissures under cyclic uniaxial increasing-amplitude decreasing-frequency (CUIADF) loads
Wang, Y.; et al.
Vol. 158, Article No. 106741, May 2022

2022/481
Metallic materials fatigue behavior: Scale levels and ranges of transition between them
Shanyavskiy, A. A.; Soldatenkov, A. P.
Vol. 158, Article No. 106773, May 2022

2022/482
Probabilistic flexural fatigue strength of ultra-lightweight cement concrete and high strength lightweight aggregate concrete
Zhang, Y.; et al.
Vol. 158, Article No. 106743, May 2022

2022/483
On the low-cycle fatigue behavior of aluminum alloys under influence of tensile pre-strain histories and strain ratio
Singh, J.; et al.
Vol. 158, Article No. 106747, May 2022

2022/484
Influence of the grain size on the fatigue initiation life curve
Mlikota, M.; et al.
Vol. 158, Article No. 106562, May 2022

2022/485
Damage evolution and probabilistic strain-lifetime assessment of plain and fiber-reinforced concrete under compressive fatigue loading: Dual and integral phenomenological model
Blasón, S.; et al.
Vol. 158, Article No. 106739, May 2022

2022/486
Estimating the fatigue behavior of a family of aluminum conductor cables using ANNs applying the Poffenberger-Swart formula
Cãmara, E. C. B.; et al.
Vol. 159, Article No. 106766, June 2022

2022/487
Multiaxial fatigue life assessment of 304 austenitic stainless steel with a novel energy-based criterion
Yang, S.; Sun, J.
Vol. 159, Article No. 106728, June 2022

2022/488
Fatigue assessment of additively-manufactured C-18150 copper alloy at room and elevated temperatures via a microstructure-sensitive algorithm
Jirandehi, A. P.; et al.
Vol. 159, Article No. 106777, June 2022

2022/489
Obtaining a lower estimate of the fatigue limit of metals by a simplified quantitative thermometric approach in a low-cost one-specimen test
Schaefer, F.; et al.
Vol. 159, Article No. 106729, June 2022

2022/490
Experimental and computational assessment of disbond growth and fatigue life of bonded joints and patch repairs for primary airframe structures
Tanulia, V.; et al.
Vol. 159, Article No. 106776, June 2022

2022/491
Investigation of the influence of a two-step process chain consisting of laser cutting and subsequent forming on the fatigue behavior of AISI 304
Wanski, T.; et al.
Vol. 159, Article No. 106779, June 2022

2022/492
Estimation of weld defects size distributions, rates and probability of detections in fabrication yards using a Bayesian theorem approach
Amirafshari, P.; Kolios, A.
Vol. 159, Article No. 106763, June 2022

2022/493
Microstructure evolution and cyclic deformation behavior of Ti-6Al-4 V alloy via electron beam melting during low cycle fatigue
Bai, C.; et al.
Vol. 159, Article No. 106784, June 2022

2022/494
A fatigue life prediction approach for laser-directed energy deposition titanium alloys by using support vector regression based on pore-induced failures
Dang, L.; et al.
Vol. 159, Article No. 106748, June 2022

2022/495
Fatigue characterization by heat source reconstruction under continuously varying stress amplitude
Douellou, C.; Balandraud, X.; Duc, E.
Vol. 159, Article No. 106782, June 2022

2022/496
Experimental insight on the fatigue resistance of FV520B-I stainless steel under corrosive environments
Wang, J.; et al.
Vol. 159, Article No. 106786, June 2022

2022/497
Synthesis of random vibration environment spectra for the fatigue analysis and optimization of railway vehicles
You, T.; et al.
Vol. 159, Article No. 106752, June 2022

2022/498
Calibration and validation of fatigue lifetime model in complex structures based on multi-level data
Liu, X.; et al.
Vol. 159, Article No. 106783, June 2022

2022/499
Effect of spindle speed during ultrasonic rolling on surface integrity and fatigue performance of Ti6Al4V alloy
Pang, Z.; et al.
Vol. 159, Article No. 106794, June 2022

2022/500
Influence of induction hardening residual stresses on rolling contact fatigue lifetime
Areitioaurtena, M.; et al.
Vol. 159, Article No. 106781, June 2022

2022/501
Inverse determination and probability distribution of the mode III strain energy density control radius with an optimized V-notched specimen under torsional fatigue loading
Benedetti, M.; et al.
Vol. 159, Article No. 106787, June 2022

2022/502
Understanding the relation between creep-fatigue fracture mechanisms and intergranular dislocation accommodation of a high chromium steel using nanoindentation characterization
Song, Y.; et al.
Vol. 159, Article No. 106796, June 2022

2022/503
Mechanical fatigue of biodegradable polymers: A study on polylactic acid (PLA), polybutylene succinate (PBS) and polybutylene adipate terephthalate (PBAT)
Zhang, J.; et al.
Vol. 159, Article No. 106798, June 2022

2022/504
Evolution of thermally induced white etching layer at rail surface during multiple wheel/train passages
Lian, Q.; et al.
Vol. 159, Article No. 106799, June 2022

2022/505
Constitutive and damage modelling of selective laser melted Ti-6Al-4V lattice structure subjected to low cycle fatigue
Zhang, P.; Zhang, D. Z.; Zhong, B.
Vol. 159, Article No. 106800, June 2022

2022/506
Dislocation-based crystal plasticity modelling of a nickel-based superalloy under dwell-fatigue: From life prediction to residual life assessment
Li, K. S.; et al.
Vol. 159, Article No. 106569, June 2022

2022/507
Effect of non-uniform microstructure on rolling contact fatigue performance of bainitic rail steel
Ruijie, Z.; et al.
Vol. 159, Article No. 106795, June 2022

2022/508
Hydrogen-accelerated white etching area formation in bearings under rolling contact fatigue
Liang, X. Z.; et al.
Vol. 159, Article No. 106753, June 2022

2022/509
A machine learning-based approach to predict the fatigue life of three-dimensional cracked specimens
Zhang, J.; et al.
Vol. 159, Article No. 106808, June 2022

2022/510
Early fatigue damage accumulation of CFRP Cross-Ply laminates considering size and stress level effects
Li, X.; Benedictus, R.; Zarouchas, D.
Vol. 159, Article No. 106811, June 2022

2022/511
Increase wind gearbox power density by means of IGS (Improved Gear Surface)
Fernandez, R. C.; Tobie, T.; Collazo, J.
Vol. 159, Article No. 106789, June 2022

2022/512
Low-cycle fatigue assessment of open-cell A332 aluminum alloy foams
Salimi, H.; et al.

Vol. 159, Article No. 106797, June 2022

2022/513
Effects of temperature and microstructure on low cycle fatigue behaviour of a PM Ni-based superalloy: EBSD assessment and crystal plasticity simulation
Zhang, W. T.; et al.
Vol. 159, Article No. 106818, June 2022

2022/514
Creep-Fatigue Response, failure mode and deformation mechanism of HAYNES 282 Ni based superalloy: Effect of dwell position and time
Mukherjee, S.; et al.
Vol. 159, Article No. 106820, June 2022

2022/515
Life evaluation of sandwich panels based on coupled creep and fatigue damage evolution
Li, W.; et al.
Vol. 159, Article No. 106819, June 2022

2022/516
Surface roughness influence in micromechanical fatigue lifetime prediction with crystal plasticity models for steel
Natkowski, E.; et al.
Vol. 159, Article No. 106792, June 2022

2022/517
An experimental investigation into fatigue behaviors of single- and double-sided U rib welds in orthotropic bridge decks
Yang, H.; et al.
Vol. 159, Article No. 106827, June 2022

2022/518
Fatigue failure mechanism of 2205 duplex stainless steel using the neutron diffraction and EBSD technologies
Zhang, W.; et al.
Vol. 159, Article No. 106828, June 2022

2022/519
Microstructure, mechanical properties and fatigue behaviors of linear friction welded weathering steels
Wang, Y.; et al.
Vol. 159, Article No. 106829, June 2022

2022/520
On the influence of cyclic loadings on the magnetic permeability of ferritic-pearlitic AISI 1045 steel
Deldar, S.; et al.
Vol. 159, Article No. 106650, June 2022

2022/521
On the changes in the low-cycle-fatigue life and cracking mechanism of P91 cross-weld specimens at elevated temperatures
Nguyen, T. T.; et al.
Vol. 159, Article No. 106833, June 2022

2022/522
Residual stress relaxation in the carburized case of austenitic stainless steel under alternating loading
Liu, Z.; et al.
Vol. 159, Article No. 106837, June 2022

2022/523
A novel excitation signal generation technology for accelerated random vibration fatigue testing based on the law of kurtosis transmission
Lei, W.; et al.
Vol. 159, Article No. 106835, June 2022

2022/524
Fatigue life prediction based on modified narrowband method under broadband random vibration loading
Wu, S. D.; et al.
Vol. 159, Article No. 106832, June 2022

2022/525
A coupled wear and crack initiation-propagation methodology for fretting fatigue life assessment in press-fitted axles
Zou, L.; et al.
Vol. 159, Article No. 106817, June 2022

2022/526
Low-cycle fatigue behavior for stainless-clad 304 + Q235B bimetallic steel
Liao, X.; et al.
Vol. 159, Article No. 106831, June 2022

2022/527
Effect of grain structure and precipitate on tensile properties and low-cycle fatigue behaviors of 2A55 Al-Cu-Li alloy
Lu, D. D.; et al.
Vol. 159, Article No. 106834, June 2022

2022/528
Generalization of the Weibull probabilistic compatible model to assess fatigue data into three domains: LCF, HCF and VHCF
Fernández-Canteli, A.; et al.
Vol. 159, Article No. 106771, June 2022

2022/529
Experimental and computational investigation of weathering steel Q450NQR1 under high cycle fatigue loading via crystal plasticity finite element method
Cong, T.; et al.
Vol. 159, Article No. 106772, June 2022

2022/530
A Structural Stress Approach Accounting for Notch Effects on Fatigue Propagation Life: Part I Theory
Yu, Y.; et al.
Vol. 159, Article No. 106793, June 2022

2022/531
Deep learning regression-based stratified probabilistic combined cycle fatigue damage evaluation for turbine bladed disks
Li, X. Q.; Song, L. K.; Bai, G. C.
Vol. 159, Article No. 106812, June 2022

2022/532
Influence of prior creep-fatigue exposure on remnant tensile and creep properties of AISI 321 austenite stainless steel
Chen, H.; et al.
Vol. 159, Article No. 106826, June 2022

2022/533
Application of machine learning algorithms for the optimization of the fabrication process of steel springs to improve their fatigue performance
Ruiz, E.; et al.
Vol. 159, Article No. 106785, June 2022

2022/534
Probabilistic fatigue modelling of metallic materials under notch and size effect using the weakest link theory
Li, X. K.; et al.
Vol. 159, Article No. 106788, June 2022

2022/535
Surface globularization generated by standard PBF-EB Ti-6Al-4V processing achieves an improvement in fatigue performance
Derimow, N.; et al.
Vol. 159, Article No. 106810, June 2022

Cement and Concrete Research
2022/536
High performance mortars from vitrified bauxite residue; the quest for the optimal chemistry and processing conditions
Giels, M.; et al.
Vol. 155, Article No. 106739, May 2022

2022/537
Effect of sulfate content and synthesis conditions on phase composition of belite-ye'elimite-ferrite (BYF) clinker
Sabbah, A.; Zhutovsky, S.
Vol. 155, Article No. 106745, May 2022

2022/538
Bio-inspired self-prestressing concrete (SPC) involving basalt fibers and expansive agent
Chu, S. H.; et al.
Vol. 155, Article No. 106735, May 2022

2022/539
Water self-diffusion in C-S-H: Effect of confinement and temperature studied by molecular dynamics
Honorio, T.; Carasek, H.; Cascudo, O.
Vol. 155, Article No. 106775, May 2022

2022/540
Transport properties of 3D printed cementitious materials with prolonged time gap between successive layers
Van Der Putten, J.; et al.
Vol. 155, Article No. 106777, May 2022

2022/541
129 Xe NMR analysis reveals efficient gas transport between inborn micro-, meso- and macropores in geopolymers
Li, J.; et al.
Vol. 155, Article No. 106779, May 2022

2022/542
Effect of alkalinity on early-age hydration in calcium sulfoaluminate clinker
Padilla-Encinas, P.; et al.
Vol. 155, Article No. 106781, May 2022

2022/543
Effect of shaping plate apparatus on mechanical properties of 3D printed cement-based materials: Experimental and numerical studies
Pan, T.; et al.
Vol. 155, Article No. 106785, May 2022

2022/544
A chemical process engineering look at digital concrete processes: critical step design, inline mixing, and scaleup
Wangler, T.; et al.
Vol. 155, Article No. 106782, May 2022

2022/545
Layer pressing in concrete extrusion-based 3D-printing: Experiments and analysis
Carneau, P.; et al.
Vol. 155, Article No. 106741, May 2022

2022/546
Capillary imbibition depth in particle-bed 3D printing – Physical frame and one-dimensional experiments
Zuo, W.; et al.
Vol. 156, Article No. 106740, June 2022

2022/547
Mechanisms affecting viscosity of cement paste made with microfines of manufactured sand
Zhu, J.; et al.
Vol. 156, Article No. 106757, June 2022

2022/548
Solidification and stabilization of strontium and chloride ions in thermally treated calcium aluminate cement modified with or without sodium polyphosphate
Irisawa, K.; et al.
Vol. 156, Article No. 106758, June 2022

2022/549
Effect of polyacrylamide on the carbonation behavior of cement paste
Zhi, F.; et al.
Vol. 156, Article No. 106756, June 2022

2022/550
Insights on chemical and physical chloride binding in blended cement pastes
Wilson, W.; et al.
Vol. 156, Article No. 106747, June 2022

2022/551
Material-process interactions in particle bed 3D printing and the underlying physics
Lowke, D.; et al.
Vol. 156, Article No. 106748, June 2022

2022/552
Atomistic simulations of ettringite and its aqueous interfaces: Structure and properties revisited with the modified ClayFF force field
Tararushkin, E. V.; Pisarev, V. V.; Kalinichev, A. G.
Vol. 156, Article No. 106759, June 2022

2022/553
Accelerated carbonation and structural transformation of blast furnace slag by mechanochemical alkali-activation
Marple, M. A. T.; et al.
Vol. 156, Article No. 106760, June 2022

2022/554
Surface area changes in C3S paste during the first drying analyzed by 1H NMR relaxometry
Maruyama, I.; et al.
Vol. 156, Article No. 106762, June 2022

2022/555
Determining hydration mechanisms for initial fall and main hydration peak in tricalcium silicate hydration using a two-scale hydration simulation model
Shen, D.; Wang, X.; Wu, S.
Vol. 156, Article No. 106763, June 2022

2022/556
Multiscale modelling of ionic diffusivity in unsaturated concrete accounting for its hierarchical microstructure
Liu, C.; Zhang, M.
Vol. 156, Article No. 106766, June 2022

2022/557
Heating cement to slow down its hydration: The unexpected role of PCE interpolymer bridge formation
Palacios, M.; et al.
Vol. 156, Article No. 106765, June 2022

2022/558
Thermodynamic equilibria-based modelling of reactive chloride transport in blended cementitious materials
Cherif, R.; et al.
Vol. 156, Article No. 106770, June 2022

2022/559
Mechanism understanding of alkali-silica reaction in alkali-activated materials system
Wang, W.; Noguchi, T.; Maruyama, I.
Vol. 156, Article No. 106768, June 2022

2022/560
The realities of additively manufactured concrete structures in practice
Bos, F. P.; et al.
Vol. 156, Article No. 106746, June 2022

2022/561
Fluid intrusion in powder beds for selective cement activation – An experimental and analytical study
Mai, I.; Lowke, D.; Perrot, A.
Vol. 156, Article No. 106771, June 2022

2022/562
Ab initio metadynamics simulations on the formation of calcium silicate aqua complexes prior to the nuleation of calcium silicate hydrate
Li, Y.; Pan, H.; Li, Z.
Vol. 156, Article No. 106767, June 2022

2022/563
Evolution of the particle size distribution of tricalcium silicate during hydration by synchrotron X-ray nano-tomography
Neubauer, J.; et al.
Vol. 156, Article No. 106769, June 2022

2022/564
Artificial neural network for the prediction of the fresh properties of cementitious materials
Charrier, M.; Ouellet-Plamondon, C. M.
Vol. 156, Article No. 106761, June 2022

2022/565
Comparison between methods for indirect assessment of buildability in fresh 3D printed mortar and concrete
Ivanova, I.; et al.
Vol. 156, Article No. 106764, June 2022

2022/566
Influence of curing temperature on the hydration and strength development of Class G Portland cement
Pang, X.; et al.
Vol. 156, Article No. 106776, June 2022

2022/567
Analysis of the trend of pH changes of concrete pore solution during the hydration by various analytical methods
Natkunarajah, K.; et al.
Vol. 156, Article No. 106780, June 2022

2022/568
Technology readiness: A global snapshot of 3D concrete printing and the frontiers for development
Ma, G.; et al.
Vol. 156, Article No. 106774, June 2022

2022/569
Molecular modeling of chemical admixtures; opportunities and challenges
Kunhi Mohamed, A.; et al.
Vol. 156, Article No. 106783, June 2022

2022/570
Influence of aluminum sulfate on properties and hydration of magnesium potassium phosphate cements
Xu, B.; et al.
Vol. 156, Article No. 106788, June 2022

2022/571
Geometric quality assurance for 3D concrete printing and hybrid construction manufacturing using a standardised test part for benchmarking capability
Buswell, R.; et al.
Vol. 156, Article No. 106773, June 2022

2022/572
Structural transition to well-ordered phases of NaOH-activated slag-metakaolin cements aged by 6 years
Burciaga-Díaz, O.; Escalante-García, J. I.
Vol. 156, Article No. 106791, June 2022

2022/573
Effect of processing on the air void system of 3D printed concrete
Das, A.; et al.
Vol. 156, Article No. 106789, June 2022

2022/574
Revisiting Tennis-Jennings method to quantify low-density/high-density calcium silicate hydrates in Portland cement pastes
Kurihara, R.; Maruyama, I.
Vol. 156, Article No. 106786, June 2022

2022/575
The first experimental evidence for improved nanomechanical properties of calcium silicate hydrate by polycarboxylate ether and graphene oxide
Li, J.; Zhang, Q.

Vol. 156, Article No. 106787, June 2022
Cement and Concrete Composites

2022/576
Improving internal curing efficiency through adjusting ab- and desorption curve of superabsorbent polymer in cement pastes using sodium carbonate
Jiang, Q.; Wan, K.
Vol. 129, Article No. 104467, May 2022

2022/577
ε–greedy automated indentation of cementitious materials for phase mechanical properties determination
Hilloulin, B.; et al.
Vol. 129, Article No. 104465, May 2022

2022/578
Synthesis and characterization of Polyethylene/B4C composite, and its neutron shielding performance in cementitious materials: Experimental and simulation studies
Park, J.; et al.
Vol. 129, Article No. 104458, May 2022

2022/579
Ultra-high-strength engineered/strain-hardening cementitious composites (ECC/SHCC): Material design and effect of fiber hybridization
Huang, B. T.; et al.
Vol. 129, Article No. 104464, May 2022

2022/580
Performance and mechanisms of stimulated self-healing in cement-based composites exposed to saline environments
Xue, C.
Vol. 129, Article No. 104470, May 2022

2022/581
Insight into dynamic compressive response of carbon nanotube/carbon fiber-reinforced concrete
Fu, Q.; et al.
Vol. 129, Article No. 104471, May 2022

2022/582
Centrifugally sprayed Engineered Cementitious Composites: Rheology, mechanics, and structural retrofit for concrete pipes
Zhu, H.; Zhang, D.; Li, V. C.
Vol. 129, Article No. 104473, May 2022

2022/583
Carbonation of cement paste with GGBFS: Effect of curing duration, replacement level and CO2 concentration on the reaction products and CO2 buffer capacity
Vanoutrive, H.; et al.
Vol. 129, Article No. 104449, May 2022

2022/584
Effect of high temperature heating on the microstructure and performance of cesium-based geopolymer reinforced by cordierite
Chen, W.; et al.
Vol. 129, Article No. 104474, May 2022

2022/585
Experimental study on static and dynamic properties of fly ash-slag based strain hardening geopolymer composites
Wang, Y.; Zhong, H.; Zhang, M.
Vol. 129, Article No. 104481, May 2022

2022/586
An RF and LSSVM–NSGA-II method for the multi-objective optimization of high-performance concrete durability
Chen, H.; et al.
Vol. 129, Article No. 104446, May 2022

2022/587
Ultraductile waterborne epoxy-concrete composite repair material: Epoxy-fiber synergistic effect on flexural and tensile performance

Pang, B.; et al.
Vol. 129, Article No. 104463, May 2022

2022/588
Effect of sodium monofluorophosphate and phosphates on mechanical properties and water resistance of magnesium oxychloride cement
Guo, Y.; Zhang, Y. X.; Soe, K.
Vol. 129, Article No. 104472, May 2022

2022/589
Hydration kinetics and microstructure development of Ultra-High Performance Concrete (UHPC) subjected to microwave pre-curing
Zhang, J.; et al.
Vol. 129, Article No. 104484, May 2022

2022/590
Effects of ladle slag on Class F fly ash geopolymer: Reaction mechanism and high temperature behavior
Luo, Y.; et al.
Vol. 129, Article No. 104468, May 2022

2022/591
Effects of synthetic CSH-tartaric acid nanocomposites on the properties of ordinary Portland cement
Li, H.; et al.
Vol. 129, Article No. 104466, May 2022

2022/592
NMR study on the early-age hydration and ion binding of the cement paste prepared with NaCl solutions
Ji, Y.; Pel, L.; Sun, Z.
Vol. 129, Article No. 104489, May 2022

2022/593
New insights into diffusion and reaction of CO2 gas in recycled aggregate concrete
Mi, R.; Liew, K. M.; Pan, G.
Vol. 129, Article No. 104486, May 2022

2022/594
Evolutions in the properties and microstructure of cement mortars containing hydroxyethyl methyl cellulose after controlling the air content
Wang, S.; et al.
Vol. 129, Article No. 104487, May 2022

2022/595
Mesoscopic simulation of crack propagation and bond behavior in ASR damaged concrete with internal/external restraint by 3D RBSM
Luo, J.; et al.
Vol. 129, Article No. 104488, May 2022

2022/596
Blending eco-efficient calcium sulfoaluminate belite ferrite cement to enhance the physico–mechanical properties of Portland cement paste cured in refrigerated and natural winter conditions
Alzaza, A.; et al.
Vol. 129, Article No. 104469, May 2022

2022/597
For the improvement of mechanical and microstructural properties of UHPC with fiber alignment using carbon nanotube and graphite nanoplatelet
Huang, H.; et al.
Vol. 129, Article No. 104462, May 2022

2022/598
Modeling of carbonation, de-carbonation and re-carbonation processes of structural concrete subjected to high temperature heating
Iwama, K.; Maekawa, K.
Vol. 129, Article No. 104493, May 2022

2022/599
Formulation of an alkali-free accelerator and its effects on hydration and mechanical properties of Portland cement
Wang, Y.; et al.
Vol. 129, Article No. 104485, May 2022

2022/600
Radiological assessment of iron silicate as a potential aggregate in concrete and mortars
Suárez-Navarro, J. A.; et al.
Vol. 129, Article No. 104490, May 2022

2022/601
Coating performance, durability and anti-corrosion mechanism of organic modified geopolymer composite for marine concrete protection
Zhang, M.; et al.
Vol. 129, Article No. 104495, May 2022

2022/602
Upcycling sintering red mud waste for novel superfine composite mineral admixture and CO2 sequestration
Liu, S.; et al.
Vol. 129, Article No. 104497, May 2022

2022/603
Incorporating PCM-enabled thermal energy storage into 3D printable cementitious composites
Brooks, A. L.; et al.
Vol. 129, Article No. 104492, May 2022

2022/604
Experimental study on gas permeability of cement-based materials
Shi, J.; et al.
Vol. 129, Article No. 104491, May 2022

2022/605
Durability and self-healing of engineered cementitious composites exposed to simulated sewage environments
Wang, T.; et al.
Vol. 129, Article No. 104500, May 2022

2022/606
Electromagnetic and mechanical properties of FA-GBFS geopolymer composite used for induction heating of airport pavement
Gu, G.; et al.
Vol. 129, Article No. 104503, May 2022

2022/607
Shrinkage prediction of recycled aggregate structural concrete with alternative binders through partial correction coefficients
Revilla-Cuesta, V.; et al.
Vol. 129, Article No. 104506, May 2022

2022/608
Image-based microstructure classification of mortar and paste using convolutional neural networks and transfer learning
Qian, H.; et al.
Vol. 129, Article No. 104496, May 2022

2022/609
Experimental investigation on torsional behaviors of ultra-high-performance fiber-reinforced concrete hollow beams
Zhou, J.; et al.
Vol. 129, Article No. 104504, May 2022

2022/610
Predicting the static yield stress of 3D printable concrete based on flowability of paste and thickness of excess paste layer
Zhang, C.; et al.
Vol. 129, Article No. 104494, May 2022

2022/611
Use of saturated lightweight sand to improve the mechanical and microstructural properties of UHPC with fiber alignment
Huang, H.; et al.
Vol. 129, Article No. 104513, May 2022

2022/612
An overview on the effect of pumping on concrete properties
Li, F.; et al.
Vol. 129, Article No. 104501, May 2022

2022/613
Damage mechanism of engineered cementitious composites after exposed to elevated temperatures: Experimental and molecular dynamics study
Zhang, J.; et al.
Vol. 129, Article No. 104507, May 2022

2022/614
Combined chelating and corrosion effects of steel fiber on the interfacial bond and tensile behaviors of ultra-high-performance concrete
Jang, Y. S.; Yoo, D. Y.
Vol. 129, Article No. 104505, May 2022

2022/615
Development of a novel compressed tablet-based bacterial agent for self-healing cementitious material
Son, Y.; et al.
Vol. 129, Article No. 104514, May 2022

2022/616
A study into the alkali-silica reactivity of recycled concrete aggregates and the role of the extent of damage in the source structures: Evaluation, accelerated testing, and preventive measures
Piersanti, M.; Shehata, M. H.
Vol. 129, Article No. 104512, May 2022

2022/617
Effect of macropores at the steel-concrete interface on localized corrosion behaviour of steel reinforcement
Wen, C.; et al.
Vol. 129, Article No. 104510, May 2022

2022/618
Influence of friction on the dynamic increase factor of concrete compressive strength in a split Hopkinson pressure bar test
Kim, K. M.; Lee, S.; Cho, J. Y.
Vol. 129, Article No. 104517, May 2022

Journal of Constructional Steel Research
2022/619
Concentric and eccentric compression performance of multiple-cell cruciform CFSTs
Hassam, M.; Guo, L.; Jia, C.
Vol. 192, Article No. 107205, May 2022

2022/620
Rotation capacity of cold-formed stainless steel RHS beams under cyclic loading
González-de-León, I.; et al.
Vol. 192, Article No. 107199, May 2022

2022/621
Trapezoidally corrugated web steel beams loaded over horizontal and inclined folds
Elamary, A. S.; et al.
Vol. 192, Article No. 107202, May 2022

2022/622
Mechanical properties of low-alloyed YSt-355-FR (0.126%Mo) cold-formed steel tube at elevated temperatures
Kumar, W.; Sharma, U. K.; Pathak, P.
Vol. 192, Article No. 107198, May 2022

2022/623
Fatigue crack growth under overload/underload in different strength structural steels
Liang, H.; et al.
Vol. 192, Article No. 107213, May 2022

2022/624
Theoretical models for T-stubs in contact with intermediate layer
Couchaux, M.; Madhouni, M.
Vol. 192, Article No. 107158, May 2022

2022/625
Seismic fragility of legged liquid storage tanks based on soil type classifications
Colombo, J. I.; Wilches, J.; Leon, R.
Vol. 192, Article No. 107212, May 2022

2022/626
Improving brace member seismic performance with amplified-deformation lever-armed dampers
Sarassantika, I. P. E.; Hsu, H. L.
Vol. 192, Article No. 107221, May 2022

2022/627
Mechanical behaviors and constitutive model of structural steel influenced by strain aging
Yang, Y.; et al.
Vol. 192, Article No. 107211, May 2022

2022/628
Seismic experimental assessment of beam-through beam-column connections for modular prefabricated steel moment frames
Du, H.; et al.
Vol. 192, Article No. 107208, May 2022

2022/629
Behaviours of column-in-column (CIC) system under axial compression: Experimental and theoretical studies
Fang, X.; et al.
Vol. 192, Article No. 107217, May 2022

2022/630
Post-earthquake fire resistance of stainless steel K-joints considering gradient temperature effect
Xu, J.; et al.
Vol. 192, Article No. 107219, May 2022

2022/631
Experimental behavior of circular composite columns with different weld arrangements
Boulaares, S.; Boutagouga, D.; Houam, A.
Vol. 192, Article No. 107229, May 2022

2022/632
Drop-weight impact tests on free from damage beam to column connections
D'Antimo, M.; Latour, M.; Demonceau, J. F.
Vol. 192, Article No. 107215, May 2022

2022/633
Development of friction-damped seismic fuses for steel storage racks
Shaheen, M. S. A.; Rasmussen, K. J. R.
Vol. 192, Article No. 107216, May 2022

2022/634
Lateral-distortional buckling of steel-concrete composite beams: Kinematics, constrained-mode GBT and analytical formulae
Araujo, H. F.; et al.
Vol. 192, Article No. 107210, May 2022

2022/635
Experimental study of U-shaped steel-concrete composite beam to square CFST column joints
Xu, X.; et al.
Vol. 192, Article No. 107220, May 2022

2022/636
DSM with different strain hardening exponent for stainless steel lipped channel columns
Chen, M.; et al.
Vol. 192, Article No. 107232, May 2022

2022/637
A novel energy dissipation damper for multi-level earthquakes
Chen, Y.; et al.
Vol. 192, Article No. 107214, May 2022

2022/638
Numerical & experimental investigation of slotted-hidden-gap connection for square HSS brace members
Afifi, M.; Tremblay, R.; Rogers, C. A.
Vol. 192, Article No. 107234, May 2022

2022/639
European seismic prequalification of steel beam-to-column joints: EQUALJOINTS and EQUALJOINTS-Plus projects
Landolfo, R.
Vol. 192, Article No. 107238, May 2022

2022/640
HSS steel corner column to H-beam joints under cyclic bidirectional loadings: Experiment, numerical modeling, and calculation
Nie, R.; et al.
Vol. 192, Article No. 107239, May 2022

2022/641
Screwed connections in built-up cold-formed steel members at ambient and elevated temperatures
Vy, S. T.; Mahendran, M.
Vol. 192, Article No. 107218, May 2022

2022/642
A partially restrained energy dissipater: Parametric analysis and application in rocking wall
Lu, Y.; Liu, Y.; Lv, Q.
Vol. 192, Article No. 107235, May 2022

2022/643
Axial compressive behaviour of high-strength steel spiral-confined square concrete-filled steel tubular columns
Yuan, F.; Cao, L.; Li, H.
Vol. 192, Article No. 107245, May 2022

2022/644
Elastic stability of unbraced plate-type modular steel frames with semi-rigid corner connections
Zhai, X.; Zha, X.; Chen, D.
Vol. 192, Article No. 107243, May 2022

2022/645
Assessment of cyclic degradation effects in composite steel-concrete members
Sahin, B.; Bravo-Haro, M. A.; Elghazouli, A. Y.
Vol. 192, Article No. 107231, May 2022

2022/646
Experimental research on the fatigue crack growth behaviour of Q420C
Chen, C. J.; et al.
Vol. 192, Article No. 107241, May 2022

2022/647
Axial compressive behavior of twining-bamboo-confined thin-walled steel tubular columns
Jin, B. B.; et al.
Vol. 192, Article No. 107246, May 2022

2022/648
Experimental study on seismic performance of column-column-beam joint in panelised steel-modular structure
Wang, H.; Zhao, X.; Ma, G.
Vol. 192, Article No. 107240, May 2022

2022/649
Seismic performance of steel corrugated plate structural walls with different corrugation inclinations
Zheng, L.; et al.
Vol. 192, Article No. 107248, May 2022

2022/650
Experimental tests of post-fire beam-column assemblies with WUF-B connections against progressive collapse
Guo, Z.; et al.
Vol. 192, Article No. 107249, May 2022

2022/651
Shaking table test of a three-story frame with resilient variable friction braces
Wang, Y.; et al.
Vol. 192, Article No. 107252, May 2022

2022/652
Seismic behavior of hollow-core infilled steel frames; an experimental and numerical study
Monfaredi, P.; Emami, S. M. M.; Moghadam, A. S.
Vol. 192, Article No. 107244, May 2022

2022/653
Design of a fuse link beam-to-column connection for earthquake resistant moment frames
Saravanan, M.; Goswami, R.; Palani, G. S.
Vol. 192, Article No. 107253, May 2022

2022/654
Experimental and numerical study on high-strength steel flange-welded web-bolted connections under fire conditions
Qiang, X.; Shu, Y.; Jiang, X.
Vol. 192, Article No. 107255, May 2022

2022/655
Design of an eccentrically buckling-restrained braced steel frame with web-bolted replaceable links
Yin, Z.; Yang, B.; Zhang, X.
Vol. 192, Article No. 107250, May 2022

2022/656
A continuous dynamic constitutive model for normal- and high-strength structural steels
Yang, X.; et al.
Vol. 192, Article No. 107254, May 2022

2022/657
Combined compression-bending performance and design of CFST with localised pitting corrosion
Li, G.; Hou, C.; Shen, L.
Vol. 192, Article No. 107247, May 2022

2022/658
Assessments on seismic performance of self-centering hybrid damping systems under far-field and near-field ground motions
Li, J.; Wang, W.
Vol. 192, Article No. 107209, May 2022

2022/659
Performance-based-plastic-design of damage-control steel MRFs equipped with self-centring energy dissipation bays
Ke, K.; et al.
Vol. 192, Article No. 107230, May 2022

2022/660
Seismic resilient steel substation with BI-TMDI: A theoretical model for optimal design
Bian, J.; et al.
Vol. 192, Article No. 107233, May 2022

2022/661
Stiffness and resistance of brace-to-upright joints with lipped channel braces assembled flange-to-flange
Gusella, F.; Orlando, M.; Peterman, K.
Vol. 193, Article No. 107258, June 2022

2022/662
Seismic behavior of through beam connection to steel box-column
Paghaleh, F. J.; Hadianfard, M. A.; Saffari, H.
Vol. 193, Article No. 107261, June 2022

2022/663
Behaviors of improved multi-cell T-shaped concrete-filled steel tubular columns under eccentric loads
Cheng, R.; et al.
Vol. 193, Article No. 107251, June 2022

2022/664
Experimental investigation on brazing residual stress distribution in 304 L stainless steel core plate
Shu, X. P.; et al.
Vol. 193, Article No. 107257, June 2022

2022/665
Structural optimization of closed built-up cold-formed steel columns
Laím, L.; et al.
Vol. 193, Article No. 107266, June 2022

2022/666
Development, seismic performance and collapse evaluation of steel moment-resisting knee braced frame
Mokhtari, M.; Islam, A.; Imanpour, A.
Vol. 193, Article No. 107262, June 2022

2022/667
Modeling methods of self-centering energy dissipation braces using OpenSees
Chen, P.; Xu, L.; Li, Z.
Vol. 193, Article No. 107267, June 2022

2022/668
Push-out tests of CFST columns strengthened with self-compacting and self-stressing concrete filled square steel tube
Huang, Y.; et al.
Vol. 193, Article No. 107263, June 2022

2022/669
Compressive behavior of circular steel tubed high-strength concrete columns with embedded steel tubes
Lu, S.; et al.
Vol. 193, Article No. 107259, June 2022

2022/670
Numerical investigation of the strength and design of cold-formed steel built-up columns
Phan. D. K.; Rasmussen, K. J. R.; Zhang, H.
Vol. 193, Article No. 107276, June 2022

2022/671
Comparative evaluation of collapse behavior at different structural levels with different connections
Zhong, W.; et al.
Vol. 193, Article No. 107280, June 2022

2022/672
Numerical evaluation on collapse-resistant performance of steel-braced concentric frames
Tan, Z.; et al.
Vol. 193, Article No. 107268, June 2022

2022/673
Experiments on welded shells with section alteration under axial and peripheral pressure
Fazlalipour, N.; Showkati, H.; Ghanbari-Ghazijahani, T
Vol. 193, Article No. 107277, June 2022

2022/674
Development of a corrugated web shear link for steel moment-resisting frames
Mansouri, A.; Mohammadzadeh Sharif, M.
Vol. 193, Article No. 107281, June 2022

2022/675
Behavior of eccentrically loaded UHPC filled circular steel tubular short columns
Wang, Q.; et al.
Vol. 193, Article No. 107282, June 2022

2022/676
Anti-collapse behavior of modular steel buildings with corrugated panels
Zhang, J. Z.; et al.
Vol. 193, Article No. 107279, June 2022

2022/677
Stability capacity design of grid cylindrical-lattice shells loaded axially
Zhu, B. L.; Guo, Y. L.; Zhang, Y. H.
Vol. 193, Article No. 107284, June 2022

2022/678
Development of a loading protocol for long links in eccentrically braced frames
Al-Janabi, M. A. Q.; Ün, E. M.; Topkaya, C.
Vol. 193, Article No. 107278, June 2022

2022/679
Post-fire performance of bonding interface in explosion-welded stainless-clad bimetallic steel
Shi, Y.; et al.
Vol. 193, Article No. 107285, June 2022

2022/680
Numerical analysis on torsional behavior of rectangular and square CFDST members
Lu, G.; et al.
Vol. 193, Article No. 107294, June 2022

2022/681
Numerical and experimental study of the BUEEP connection using an inner box
Rafiei Tekieh, S. M.; Zandi, A. P.; Pashaei, M. H.
Vol. 193, Article No. 107264, June 2022

2022/682
Numerical modelling and equivalent brace model of cold-formed steel buckling-restrained steel plate shear walls
Tan, J. K.; et al.
Vol. 193, Article No. 107289, June 2022

2022/683
Double skin composite beams at Arctic low temperatures: Numerical and analytical studies
Yan, J. B.; et al.
Vol. 193, Article No. 107286, June 2022

2022/684
Shear buckling behavior of tapered cantilever beams with corrugated trapezoidal web under concentrated tip load
Shariatyazdi, P.; et al.
Vol. 193, Article No. 107265, June 2022

2022/685
Experimental and numerical investigation of a novel all-steel assembled core-perforated buckling-restrained brace
Yun, Z.; et al.
Vol. 193, Article No. 107288, June 2022

2022/686
Experimental and analytical investigation of stiffened steel tubes for wind turbine towers under compression-bending load
Ren, W.; et al.
Vol. 193, Article No. 107296, June 2022

2022/687
Development of bent shear panel dampers for eccentrically braced composite frames
Zhao, J. Z.; tao, M. X.; Zhuang, L. D.
Vol. 193, Article No. 107292, June 2022

2022/688
Optimal allocation of material and slenderness limits for the rectangular concrete-filled columns
Saleh, E.; Alghossoon, A.; Tarawneh, A.
Vol. 193, Article No. 107283, June 2022

2022/689
Determination of high-temperature creep and post-creep response of structural steels
Wu, Z.; et al.
Vol. 193, Article No. 107287, June 2022

2022/690
Seismic performance of braced frame with double round steel tube
Zheng, L.; et al.
Vol. 193, Article No. 107297, June 2022

2022/691
Design of cold-formed steel battened built-up columns
Dar, M. A.; et al.
Vol. 193, Article No. 107291, June 2022

2022/692
Experimental study on torsional behaviour of square concrete filled CFRP-steel tube (S-CF-CFRP-ST)
Kuan, P.; et al.

Vol. 193, Article No. 107295, June 2022

Composites Part B: Engineering

2022/693

PAN/W18O49/Ag nanofibrous membrane for high-efficient and multi-band electromagnetic-interference shielding with broad temperature tolerance and good thermal isolating capacity
Wang, H.; et al.
Vol. 236, Article No. 109793, May 2022

2022/694

Ionic liquid-based non-releasing antibacterial, anti-inflammatory, high-transparency hydrogel coupled with electrical stimulation for infected diabetic wound healing
Liu, B.; et al.
Vol. 236, Article No. 109804, May 2022

2022/695

Sustained gene delivery from inflammation-responsive anti-inflammatory hydrogels promotes extracellular matrix metabolism balance in degenerative nucleus pulposus
Wang, Y.; et al.
Vol. 236, Article No. 109806, May 2022

2022/696

A careob-like nanofibers with a sustained drug release profile for promoting skin wound repair and inhibiting hypertrophic scar
Zhang, H.; et al.
Vol. 236, Article No. 109790, May 2022

2022/697

Highly smooth, robust, degradable and cost-effective modified lignin-nanocellulose green composite substrates for flexible and green electronics
Jia, D.; et al.
Vol. 236, Article No. 109803, May 2022

2022/698

Gastric fluid-induced double network hydrogel with high swelling ratio and long-term mechanical stability
Jin, X.; et al.
Vol. 236, Article No. 109816, May 2022

2022/699

Engineering titanium carbide ultra-thin nanosheets for enhanced fire safety of intumescent flame retardant polylactic acid
Shi, Y.; et al.
Vol. 236, Article No. 109792, May 2022

2022/700

Characterizing friction for fiber reinforced composites manufacturing: Method development and effect of process parameters1
Das, A.; et al.
Vol. 236, Article No. 109777, May 2022

2022/701

Structural design and optimization of metal-organic framework-derived FeOx@C/rGO anode materials for constructing high-performance hybrid supercapacitors
Sun, L.; et al.
Vol. 236, Article No. 109812, May 2022

2022/702

Superior strength-ductility synergy in a novel tailored Zr-based particle-strengthened medium W content alloys
Li, Z. B.; et al.
Vol. 236, Article No. 109817, May 2022

2022/703

An injectable and conductive TEMPOL/polypyrrole integrated peptide co-assembly hydrogel promotes functional maturation of cardiomyocytes for myocardial infarction repair
Zhan, J.; et al.
Vol. 236, Article No. 109794, May 2022

2022/704
Cost-effective graphite felt and phosphorous flame retardant with extremely high electromagnetic shielding
Yin, Z.; et al.
Vol. 236, Article No. 109819, May 2022

2022/705
Covalent treatment of carbon fibre with functionalized MoS2 nanosheets using thiol-ene click chemistry: The improvement of interface in multiscale epoxy composites
Ahmadi, M.; et al.
Vol. 236, Article No. 109821, May 2022

2022/706
Duplex strengthening via SiC addition and in-situ precipitation in additively manufactured composite materials
Tan, C.; et al.
Vol. 236, Article No. 109820, May 2022

2022/707
Mechanical properties and energy absorption of bio-inspired hierarchical circular honeycomb
Ha, N. S.; et al.
Vol. 236, Article No. 109818, May 2022

2022/708
3D printed tubular lattice metamaterials for mechanically robust stents
Jiang, H.; et al.
Vol. 236, Article No. 109809, May 2022

2022/709
Ultrahigh augmentation of flexible composite-based piezoelectric energy harvesting efficiency via polymer-impregnated nanoparticles network within 3D cellulose scaffold
Zhang, H.; et al.
Vol. 236, Article No. 109813, May 2022

2022/710
Synergistic effect of cementite amorphization and oxidation on forming a nanocomposite self-lubricating surface during sliding
Yin, C. H.; et al.
Vol. 236, Article No. 109799, May 2022

2022/711
An ultrastrong bioinspired soy protein isolate-based nanocomposite with graphene oxide intercalation
Liu, T.; et al.
Vol. 236, Article No. 109805, May 2022

2022/712
Natural rosin-grafted nanoparticles for extremely-robust and eco-friendly antifouling coating with controllable liquid transport
Qing, Y.; et al.
Vol. 236, Article No. 109797, May 2022

2022/713
Energy conversion and storage using artificially induced antiferroelectricity in HfO2/ZrO2 nanolaminates
Yang, K.; et al.
Vol. 236, Article No. 109824, May 2022

2022/714
Towards in-situ acoustic emission-based health monitoring in bio-based composites structures: Does embedment of sensors affect the mechanical behaviour of flax/epoxy laminates?
Seychal, G.; et al.
Vol. 236, Article No. 109787, May 2022

2022/715
Diamond-like carbon coating and surface grafting of osteoprotegerin and alendronate on polyetheretherketone to ameliorate the mechanical performance and osseointegration simultaneously
Chen, J.; et al.
Vol. 236, Article No. 109815, May 2022

2022/716
Experimental and 3D mesoscopic investigation of uniaxial compression performance on basic magnesium sulfate cement-coral aggregate concrete (BMSC-CAC)
Guo, J.; et al.
Vol. 236, Article No. 109760, May 2022

2022/717
Interfacial engineering of ZIF-67 derived CoSe/Co(OH)2 catalysts for efficient overall water splitting
Li, C. G. W.; et al.
Vol. 236, Article No. 109823, May 2022

2022/718
Micromechanics-based phase field fracture modelling of CNT composites
Quinteros, L.; García-Macías, E.; Martínez-Pañeda, E.
Vol. 236, Article No. 109788, May 2022

2022/719
Anisotropy-inspired, simulation-guided design and 3D printing of microlattice metamaterials with tailored mechanical-transport performances
Zhang, L.; et al.
Vol. 236, Article No. 109837, May 2022

2022/720
A feather-inspired interleaf for enhanced interlaminar fracture toughness of carbon fiber reinforced polymer composites
Song, W.; et al.
Vol. 236, Article No. 109827, May 2022

2022/721
Multifunctional sandwich-structured magnetic-electric composite films with Joule heating capacities toward absorption-dominant electromagnetic interference shielding
Guo, Z.; et al.
Vol. 236, Article No. 109836, May 2022

2022/722
Ternary assembled MOF-derived composite: Anisotropic epitaxial growth and microwave absorption
Wu, F.; et al.
Vol. 236, Article No. 109839, May 2022

2022/723
Ferrocenyl-containing silicone nanocomposites as materials for neuronal interfaces
Deriabin, K. V.; et al.
Vol. 236, Article No. 109838, May 2022

2022/724
Combining advanced 3D printing technologies with origami principles: A new paradigm for the design of functional, durable, and scalable springs
Khazaaleh, S.; Masana, R.; Daqaq, M. F.
Vol. 236, Article No. 109811, May 2022

2022/725
Improvement on strength and toughness for CFRPs by construction of novel “soft-rigid” interface layer
Pu, Y.; et al.
Vol. 236, Article No. 109846, May 2022

2022/726
The effects of cations and concentration on reaction mechanism of alkali-activated blast furnace ferronickel slag
Huang, Z.; Wang, Q.; Lu, J.
Vol. 236, Article No. 109825, May 2022

2022/727
Rapid fiber alignment quantification in direct write printing of short fiber reinforced composites
Wright, W. J.; et al.
Vol. 236, Article No. 109814, May 2022

2022/728
Effect of equienergetic low-velocity impact on CFRP with surface ice in low temperature arctic conditions
Banik, A.; et al.
Vol. 236, Article No. 109850, May 2022

2022/729
Heterostructures of mixed metal oxides (ZnMnO3/ZnO) synthesized by a wet-chemical approach and their application for the electrochemical detection of the drug chlorpromazine
Balamurugan, K.; et al.
Vol. 236, Article No. 109822, May 2022

2022/730
Effects of natural aging on precipitation behavior and hardening ability of peak artificially aged SiCp/Al-Mg-Si composites
Zhu, S. Z.; et al.
Vol. 236, Article No. 109851, May 2022

2022/731
Remote-controllable, tough, ultrastretchable, and magneto-sensitive nanocomposite hydrogels with homogeneous nanoparticle dispersion as biomedical actuators, and their tuned structure, properties, and performances
Han, W. J.; et al.
Vol. 236, Article No. 109802, May 2022

2022/732
Comfort fitting shape memory elastomer with constructed strong interface based on amphiphilic hybrid Janus particles
Hu, J.; et al.
Vol. 236, Article No. 109828, May 2022

2022/733
Enhanced ohmic heating and chloride adsorption efficiency of conductive seawater cementitious composite: Effect of non-conductive nano-silica
Tian, W.; Liu, Y.; Wang, W.
Vol. 236, Article No. 109854, May 2022

2022/734
Effects of carbon nanotube-polydopamine hybridization on the mechanical properties of short carbon fiber/polyetherimide composites
Sun, Z.; et al.
Vol. 236, Article No. 109848, May 2022

2022/735
Red blood cell-like magnetic particles and magnetic field promoted neuronal outgrowth by activating Netrin-1/DCC signaling pathway in vitro and in vivo
Liu, M.; et al.
Vol. 237, Article No. 109789, May 2022

2022/736
Hierarchically porous N-doped C nanofibers comprising TiO2 quantum dots and ZIF-8-derived hollow C nanocages as ultralight interlayer for stable Li–S batteries
Seon, Y. H.; Saroha, R.; Cho, J. S.
Vol. 237, Article No. 109856, May 2022

2022/737
Shock resistance of elastomer-strengthened metallic corrugated core sandwich panels
Wang, X.; et al.
Vol. 237, Article No. 109840, May 2022

2022/738
Multi-physics design of a new battery packaging for electric vehicles utilizing multifunctional composites
Pejman, R.; Gorman, J.; Najafi, A. R.
Vol. 237, Article No. 109810, May 2022

2022/739
Enhanced optical nonlinearity and ultrafast carrier dynamics of TiO2/CuO nanocomposites
Dong, L.; et al.
Vol. 237, Article No. 109860, May 2022

2022/740
Novel exploration of the flame retardant potential of bimetallic MXene in epoxy composites
Gong, K.; et al.
Vol. 237, Article No. 109862, May 2022

2022/741
Magnetic-driven wireless electrical stimulation in a scaffold
Qi, F.; et al.
Vol. 237, Article No. 109864, May 2022

2022/742
Deformation and failure of pseudo-ductile quasi-isotropic all-carbon hybrid FRPS with an open hole under tension
Sapozhnikov, S. B.; et al.
Vol. 237, Article No. 109870, May 2022

2022/743
Prediction and analysis of properties of ramie fiber staple yarn reinforced unsaturated polyester composite based on fiber packing density
Zuo, Q.; et al.
Vol. 237, Article No. 109869, May 2022

2022/744
Investigation on air blast resistance of POZD-coated composite steel plates: Experiment and numerical analysis
Wang, W.; et al.
Vol. 237, Article No. 109858, May 2022

2022/745
Magnetic ZrO2/PEI/Fe3O4 functionalized MWCNTs composite with enhanced phosphate removal performance and easy separability
Liu, X.; et al.
Vol. 237, Article No. 109861, May 2022

2022/746
Stretchable translucent nanocomposite membranes with 3D heterogeneous interfaces derived from sugar templates for mechano-responsive optical applications
Yun, S.; et al.
Vol. 237, Article No. 109852, May 2022

2022/747
Internal low-velocity impact damage prediction in CFRP laminates using surface profiles and machine learning
Hasebe, S.; et al.
Vol. 237, Article No. 109844, May 2022

2022/748
Enhanced interfacial properties of hierarchical MXene/CF composites via low content electrophoretic deposition
Hu, Y.; et al.
Vol. 237, Article No. 109871, May 2022

2022/749
Matrix–fiber interfacial debonding in soft composite materials: Cyclically behavior modeling and microstructural evolution
Mansouri, M. R.; et al.
Vol. 237, Article No. 109853, May 2022

2022/750
Neutrophil-erythrocyte hybrid membrane-coated hollow copper sulfide nanoparticles for targeted and photothermal/ anti-inflammatory therapy of osteoarthritis
Xue, X.; et al.
Vol. 237, Article No. 109855, May 2022

2022/751
Anisotropy in conventional and uniaxially thermoformed auxetic polymer foams
Zhang, Q.; et al.
Vol. 237, Article No. 109849, May 2022

2022/752
Supramolecular hydrogel-loaded Prussian blue nanoparticles with photothermal and ROS scavenging ability for tumor postoperative treatments
Tong, Z.; et al.
Vol. 237, Article No. 109872, May 2022

2022/753
Waterproof geopolymer composites modified by hydrophobic particles and polydimethylsiloxane
Ruan, S.; et al.
Vol. 237, Article No. 109865, May 2022

2022/754
Experimental investigation into influences of Z-pin and deltoid on structural properties and damage tolerance of CFRP T-joints
Zhou, J.; et al.
Vol. 237, Article No. 109875, May 2022

2022/755
Strain-rate dependent mode I cohesive traction laws for glass fiber-epoxy interphase using molecular dynamics simulations
Chowdhury, S. C.; Gillespie, J. W.
Vol. 237, Article No. 109877, May 2022

2022/756
Construction of sphere like samarium vanadate nanoparticles anchored graphene nanosheets for enhanced electrochemical detection of nitrofurantoin in biological fluids
Babulal, S. M.; et al.
Vol. 237, Article No. 109847, May 2022

2022/757
Synergistic fracture toughness enhancement of epoxy-amine matrices via combination of network topology modification and silica nanoparticle reinforcement
Gao, J.; et al.
Vol. 238, Article No. 109857, June 2022

2022/758
Stress field prediction in fiber-reinforced composite materials using a deep learning approach
Bhaduri, A.; Gupta, A.; Graham-Brady, L.
Vol. 238, Article No. 109879, June 2022

2022/759
Depth of penetration experiments of S-2 glass/epoxy composites: A new Experimental Methodology in determining the rate dependent dynamic crush strength of composites (Gama)
Haque, B. Z.; Kubota, M.; Gillespie, J. W.
Vol. 238, Article No. 109917, June 2022

2022/760
Pearlite formation via martensite
Li, S.; et al.
Vol. 238, Article No. 109859, June 2022

2022/761
Dual-mode biomimetic soft actuator with electrothermal and magneto-responsive performance
Li, W.; et al.
Vol. 238, Article No. 109880, June 2022

2022/762
Label-free electrochemical immunosensor based on l-cysteine-functionalized AuNP on reduced graphene oxide for the detection of dengue virus E-protein in dengue blood serum
Sangili, A.; et al.
Vol. 238, Article No. 109876, June 2022

2022/763
Antimicrobial, UV blocking, water-resistant and degradable coatings and packaging films based on wheat gluten and lignocellulose for food preservation
Chen, Y.; et al.
Vol. 238, Article No. 109868, June 2022

2022/764
Technological improvement rates and recent innovation trajectories in automated advanced composites manufacturing technologies: A patent-based analysis
Alves de Campos, A.; Henriques, E.; Magee, C. L.
Vol. 238, Article No. 109888, June 2022

2022/765
Electroluminescent strain sensing on carbon fiber reinforced polymer
Qiu, J.; et al.
Vol. 238, Article No. 109893, June 2022

2022/766
Design, manufacturing and FEA prediction of the mechanical behavior of a hybrid-molded polycarbonate / continuous carbon fiber reinforced composite component
Monti, M.; et al.
Vol. 238, Article No. 109891, June 2022

2022/767
Experimental investigations on phenomenological constitutive model of closed-cell PVC foam considering the effects of density, strain rate and anisotropy
Tang, Y.; et al.
Vol. 238, Article No. 109885, June 2022

2022/768
Design of zero thermal expansion and high thermal conductivity in machinable xLFCS/Cu metal matrix composites
Pang, X.; et al.
Vol. 238, Article No. 109883, June 2022

2022/769
Assessment of performance degradation of hybrid flax-glass fiber reinforced epoxy composites during a salt spray fog/dry aging cycle
Fiore, V.; et al.
Vol. 238, Article No. 109897, June 2022

2022/770
Hydrogen-bonded quasi-layered polypyrrole-tungstate complex with exceptional electrochemical capacitance over 25000 cycles
Liu, H.; et al.
Vol. 238, Article No. 109910, June 2022

2022/771
A hybrid method for determination of fatigue limit and non-destructive evaluation of composite structures after low-velocity impact loading
Katunin, A.; et al.
Vol. 238, Article No. 109898, June 2022

2022/772
Study on the floating kinetics of graphene in molten Sn-based alloy based on in-situ observation of X-ray radiography
Li, Y.; et al.
Vol. 238, Article No. 109909, June 2022

2022/773
Highly conductive ZrO2–x spheres as bifunctional framework stabilizers and gas evolution relievers in nickel-rich layered cathodes for lithium-ion batteries
Kim, Y. J.; et al.
Vol. 238, Article No. 109911, June 2022

2022/774
Multifunctional cellular sandwich structures with optimised core topologies for improved mechanical properties and energy harvesting performance
Chen, B.; et al.
Vol. 238, Article No. 109899, June 2022

2022/775
High thermal conductivity in diamond induced carbon fiber-liquid metal mixtures
Zeng, C.; Ma, C.; Shen, J.
Vol. 238, Article No. 109902, June 2022

2022/776
Electrospinning of PVP-based ternary composites containing SiO2 nanoparticles and hybrid TiO2 microparticles with adsorbed superoxide radicals
Passaro, J.; et al.
Vol. 238, Article No. 109874, June 2022

2022/777
High-temperature oxidation behavior and mechanism of the Si-based thermal protective coating for SiCf/SiC composites under static oxidation and H2O/O2/Na2SO4 corrosion oxidation
Quan, H.; et al.
Vol. 238, Article No. 109906, June 2022

2022/778
Sodium-deficient O3–Na0.75Fe0.5-xCuxMn0.5O2 as high-performance cathode materials of sodium-ion batteries
Wei, T. T.; et al.
Vol. 238, Article No. 109912, June 2022

2022/779
Innovative design of hierarchical cobalt-based borate functionalized black phosphorus structure with petal-like wrinkle: Enhancing the fire safety and mechanical properties of epoxy resin
Zhou, Y.; et al.
Vol. 238, Article No. 109886, June 2022

2022/780
Processing, thermal conductivity and flame retardant properties of silicone rubber filled with different geometries of thermally conductive fillers: A comparative study
Li, Y. T.; et al.
Vol. 238, Article No. 109907, June 2022

2022/781
Synthesis of waterborne polyurethane by inserting polydimethylsiloxane and constructing dual crosslinking for obtaining the superior performance of waterborne coatings
Li, F.; et al.
Vol. 238, Article No. 109889, June 2022

2022/782
Efficient Co–Ni oxysulfide nanoarchitectured materials for long-lasting electrochemical cells: Biodegradable parafilm assisted pouch-type cells for portable electronic applications
Ramulu, B.; Arbaz, S. J.; Yu, J. S.
Vol. 238, Article No. 109915, June 2022

2022/783
Super-stretchable polymer-AgPdCu superlattice electrodes for high-performance wearable electronics
Sim, H. M.; et al.
Vol. 238, Article No. 109914, June 2022

2022/784
Robust bioactive protein-based screws with dual crosslinked network for internal bone fixation
Zhang, Q. C.; et al.
Vol. 238, Article No. 109884, June 2022

2022/785
Synergistic effect of cellulose nanocrystals-graphene oxide as an effective nanofiller for enhancing properties of solventless polymer nanocomposites
Dhamodharan, D.; et al.
Vol. 238, Article No. 109918, June 2022

2022/786
Design and manufacture of thermoplastic carbon fiber/polyethylene terephthalate composites underbody shield to protect the lithium-ion batteries for electric mobility from ground impact
Um, H. J.; et al.
Vol. 238, Article No. 109892, June 2022

2022/787
Arbitrarily shapeable and conductive hydrogel with “Magic Cube” like structure for real-time monitoring and promoting wound healing
Chen, F.; et al.
Vol. 238, Article No. 109903, June 2022

2022/788
Chloride binding behavior of synthesized reaction products in alkali-activated slag
Cai, W.; et al.
Vol. 238, Article No. 109919, June 2022

2022/789
In situ study on fracture behaviors of SiC/2A14Al composite joint : Co-construction of microstructure and mechanical properties via laser welding
Zhang, M.; et al.
Vol. 238, Article No. 109882, June 2022

2022/790
High-performance flame-retardant polycarbonate composites: Mechanisms investigation and fire-safety evaluation systems establishment
Mu, X.; et al.
Vol. 238, Article No. 109873, June 2022

2022/791
A simple and universal strategy for construction and application of silica-based flame-retardant nanostructure
Qiu, X.; et al.
Vol. 238, Article No. 109887, June 2022

2022/792
Novel enzyme-sensitive poly-tioxolone membranes for peritendinous anti-adhesion
Li, Y.; et al.
Vol. 238, Article No. 109904, June 2022

2022/793
A bio-inspired foam-filled multi-cell structural configuration for energy absorption
Yao, R.; et al.
Vol. 238, Article No. 109801, June 2022

2022/794
Preparation and mechanism study of a high efficiency bio-based flame retardant for simultaneously enhancing flame retardancy, toughness and crystallization rate of poly (lactic acid)
Xu, Y.; et al.
Vol. 238, Article No. 109913, June 2022

2022/795
Architected cellular fiber-reinforced composite
Estakhrianhaghighi, E.; et al.
Vol. 238, Article No. 109894, June 2022

2022/796
On mode-I and mode-II interlaminar crack migration and R-curves in carbon/epoxy laminates with hybrid toughening via core-shell rubber particles and thermoplastic micro-fibre veils
Akbolat, M. Ç.; et al.
Vol. 238, Article No. 109900, June 2022

2022/797
Electrospun biodegradable nanofibers loaded with epigallocatechin gallate for guided bone regeneration
Song, L.; et al.
Vol. 238, Article No. 109920, June 2022

2022/798
Targeted modification of black phosphorus by MIL-53(Al) inspired by “Cannikin's Law” to achieve high thermal stability of flame retardant polycarbonate at ultra-low additions
Qian, Z.; et al.
Vol. 238, Article No. 109943, June 2022

2022/799
β-CD/PEI/PVA composite hydrogels with superior self-healing ability and antibacterial activity for wound healing
Liu, D.; et al.
Vol. 238, Article No. 109921, June 2022

2022/800
Simultaneous improvements of the fire safety, mechanical properties and water resistance of vinyl ester resin composites by introducing microencapsulated ammonium polyphosphate by polytriazole
Du, H.; et al.
Vol. 238, Article No. 109908, June 2022

2022/801
Qualitative and quantitative analysis of neutron irradiation effects in SiC/SiC composites using X-ray computed tomography
Arregui-Mena, J. D.; et al.
Vol. 238, Article No. 109896, June 2022

2022/802
Adjustable brittle-ductile transition behavior and rheological behavior of polypropylene random copolymer nanocomposites through well interfacial-loaded nanoparticles
Zhao, S.; et al.
Vol. 238, Article No. 109939, June 2022

2022/803
A facile, biosynthetic design strategy for high-performance multifunctional bacterial cellulose-based dressing
Yang, Z.; et al.
Vol. 238, Article No. 109945, June 2022

2022/804
A novel filler of biocomposites for long-term self-regulated delivery of immunomodulatory and antibacterial components to accelerate bone regeneration
Min, H.; et al.
Vol. 238, Article No. 109942, June 2022

2022/805
Sustainable plastic composites by polylactic acid-starch blends and bleached kraft hardwood fibers
Serra-Parareda, F.; et al.
Vol. 238, Article No. 109901, June 2022

2022/806
P-doped PANI/AgMWs nano/micro coating towards high-efficiency flame retardancy and electromagnetic interference shielding
Zhang, L.; et al.
Vol. 238, Article No. 109944, June 2022

2022/807
Preservation of cardiac functions post myocardial infarction in vivo by a phenylboric acid-grafted hyaluronic hydrogel with anti-oxidation and accelerated degradation under oxidative microenvironment
Wang, S.; et al.
Vol. 238, Article No. 109941, June 2022

2022/808
A bioprosthetic heart valve prepared by copolymerization of 2-isocyanatoethyl methacrylate modified pericardium and functional monomer
Zheng, C.; et al.
Vol. 238, Article No. 109922, June 2022

2022/809
Nanotextured surfaces with enhanced ice-traction and wear-resistance
Namdari, N.; et al.
Vol. 238, Article No. 109916, June 2022

2022/810
In situ elastic constant determination of unidirectional CFRP composites via backwall reflected multi-mode ultrasonic bulk waves using a linear array probe

Cao, H.; et al.
Vol. 238, Article No. 109953, June 2022

2022/811
Superior superplasticity and multiple accommodation mechanisms in TiB reinforced near-α titanium matrix composites
Qiu, P.; et al.
Vol. 238, Article No. 109940, June 2022

2022/812
Multi-hierarchical earbuds-ball-like silicon suboxide-carbon hybrids design for high-performance lithium storage
Yang, Z.; et al.
Vol. 238, Article No. 109951, June 2022

2022/813
Hybrid nanoparticles based on novel Schiff Base for durable flame retardant and antibacterial properties
Li, N.; et al.
Vol. 238, Article No. 109905, June 2022

2022/814
A one-photon excitation pathway in 0D/3D CoS2/ZnIn2S4 composite with nanoparticles on micro-flowers structure for boosted visible-light-driven photocatalytic hydrogen evolution
Cai, Y.; et al.
Vol. 238, Article No. 109955, June 2022

CSIR-SERC RESEARCH HIGHLIGHTS

Sponsored Research Project	Evaluation and management of longitudinal force on substructures of railway bridges April 2017- December 2020

Project Leader

Dr K.Kesavan

Dr Ing Saptarshi Sasmal

Team

Prof Santosh Kapuria
Dr Balaji Rao
Dr Parivallal S
Dr Srinivas V
Dr Anandavalli N
Dr Arun Sundaram B
Dr Lakshmi K
Mr Saravana Kumar
Dr Nawal Kishor Banjara
Dr B.S.Sindu
Mr M.Kannusamy
Ms A.Thirumalai Selvi

Sponsoring Agency: Research Designs & Standards Organisation, Lucknow

Objectives Achieved/ Progress made:

The main aim of this project is to evaluate the longitudinal force coming on the railway bridge sub structure due to the passage of trains. Experimental investigations at laboratory was carried out to understand dispersion of longitudinal forces in railway bridges. Experimental investigations were carried out on three bridges 60 (PSC box girder), 145 (steel plate girder) and 1584 (steel plate girder) for the evaluation of longitudinal forces (Figs. 1). Instrumentation of the bridge was carried out using strain gages, displacement transducers and accelerometers. Dynamic tests were carried out using special train formation as per RDSO guidelines and responses were measured. Finite element simulations were also carried out to study the behaviour under different loading conditions.

Bridge 1584

Bridge 60

Bridge 145

Fig. 1 Instrumentation and testing of different Bridges

Benefits likely to accrue to the sponsor on completion of project:

The measured longitudinal force will be useful for the effective design of railway bridges.

Sponsored Research Project	Testing and evaluation of AAR-H coupler with draft gear assembly November 2018- May-2019

Project Leader

Shri G. Ramesh

Team

Dr P.S. Ambily

Sponsoring Agency: M/s. Escorts Railway Equipment Division

Objective Achieved/ Progress made:

The AAR-H tight lock coupler and draft gear supplied by M/s. Voith Turbo India Private Limited, Hyderabad were tested for static load displacement characteristics in tension and compression modes, compressive proof load of 2000 kN, tensile proof load of 1000 kN and tensile fracture load of 1500 kN. There was no permanent deformation at compression and tension proof loads and the strains were within the elastic limit of 0.2%. No fracture deformation observed at 1500 kN tensile load in AAR-H coupler. The draft gear and coupler assembly (duly strain gauged) were mounted on the test fixture and erected on the testing machine in vertical position as shown in Fig.1 a and b. The coupler assembly was subjected to bending proof load of 300 kN and bending fracture load of 500 kN. There was no permanent deformation at bending proof load and the strains were within the elastic limit of 0.2%. No fracture deformation observed at 500 kN bending load.

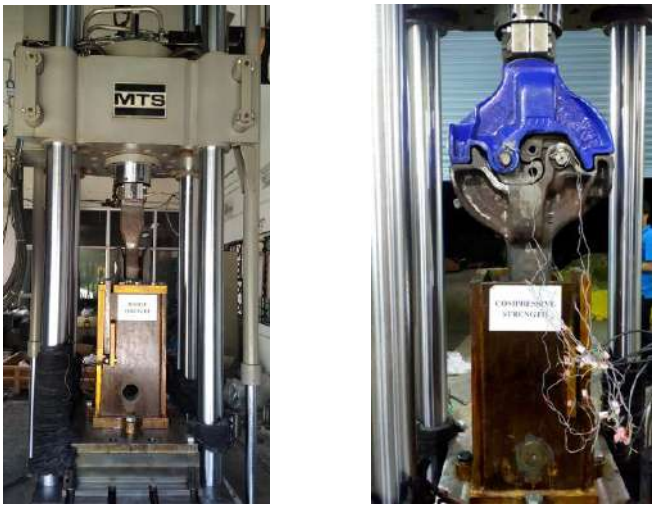

(a) (b)

Fig. 1 View of typical test setup of draft gear and coupler assembly

Benefits likely to accrue to the sponsor on completion of project:

Testing of locomotive coupler and draft gear assemblies will be beneficial to Indian Railways to improve and ensure the passenger safety in existing coaches and newly developed coaches.

Sponsored Research Project	Condition assessment and performance evaluation of four number of bridges at VPT and formulation of remedial measures January 2019 - July 2019

Project Leader

Dr V. Srinivas

Team

Prof Santosh Kapuria
Dr Ing Saptarshi Sasmal
Dr S. Parivallal
Dr K. Kesavan
Dr B. Arun Sundaram
Shri. K. Saravana Kumar
Dr Nawal Kishor Banjara
Dr B.S.Sindu

Sponsoring Agency: Visakhapatnam Port Trust, Visakhapatnam, A.P

Objective Achieved/ Progress made:

Visual inspection was carried out on all the four bridge sites viz. Ambedkar Centenary flyover bridge and NHAI bridge Nehru Centenary flyover bridge, Sardharvallabai Patel Parallel bridge, Bowstring girder bridge on IBP road and some major observations were made. Instrumentations were carried out at different locations of the bridges for strain, deflection and vibration response measurement. A tripper truck (with different load cases) was positioned at different locations on the bridge span and the strain and deflection responses obtained at critical locations under these load cases was measured. Then, numerical models of the bridges were simulated using the information provided in the drawings and site measurements. The deflection response obtained from the numerical model at the critical locations under different load cases (considered in the field investigations) is validated with the field measurements. IRC loading is then applied on the validated numerical models and checked for safety. Figures1(a) & 1(b) show the general view, distresses in bridges, instrumentations and loading of the bridges. From the visual, field and numerical investigations of the bridges, some alarming sign of distresses in bearings, pier cap, pedestal, rupture of prestressing cable are envisaged. Inorder to improve the condition and rating of the bridge structure and to continue the normal traffic, recommendations are provided along with traffic load restrictions and further appropriate suitable repair/retrofitting schemes were recommended.

(a) (b)

Fig. 1 General view of the bridges

Benefits likely to accrue to the sponsor on completion of project:

The recommendations will be useful for repair and retrofitting of distressed members, which in turn will enhance the service life of the bridges.

Sponsored Research Project	Experimental studies to investigate the efficacies of induction furnace slag as a substitute for river sand February 2019 - June 2019

Sponsoring Agency: Agni Steels Private Ltd. Erode, Tamil Nadu

Project Leader

Dr T. Hemalatha

Team

Dr B.S Sindu

Objective Achieved/ Progress made:

The main objective of this work is to find the feasibility of using this slag fine aggregate as an alternative to conventional river sand/M sand. Experimental investigations carried out on the aggregate prepared from the slag, a steel industry waste is presented in this study. Initially, the as received slag has been crushed to the fine aggregate size as shown in Fig. 1 and detailed study has been carried out on the slag aggregate.

Total of six concrete mixes with two types of cement (OPC and PPC) and three types of aggregates have been made for this study. Comprehensive study has been carried out on the slag aggregate as well as on the concrete made using slag aggregate. Water absorption test, one of the important properties for slag aggregate carried out in this study is shown in Fig. 2.

The essential properties such as mechanical and durability characteristics which determine the quality of the concrete is obtained. It is found that the mechanical properties and durability characteristics obtained for the concrete made with slag aggregate is comparable with that of the concrete made with river sand and M-sand.

Fig. 1 a) As received b) Crushed in jaw crusher c) Crushed aggregate passed in 2.36 mm sieve

Fig. 2. Water absorption test a) Slag aggregate immersed in water b) Slag aggregate in saturated surface dry condition c) Aggregate in oven

Benefits likely to accrue to the sponsor on completion of project:

The fine aggregate made using the slag aggregate can be used as an alternative for river sand.

Sponsored Research Project	Condition assessment of cooling water pump house, clarifloculator, water treatment plant and DM pre-treatment plant (Phase -III) February 2019 – May 2019

Project Leader

Dr S. Bhaskar

Team

Dr A. Kanchana Devi
Shri Bhashya Vankudothu

Sponsoring Agency: M/s. NTPC Ltd., Ramagundam, Telangana

Objectives Achieved/ Progress made:

The present condition of identified structures were assessed systematically by carrying out in-situ non-destructive testing (NDT). Detailed visual observation was carried out on cooling water pump house, Clarifloculator, Water treatment/pretreatment plant (PTP) and DM pre-treatment plant. Rebond hammer and Ultrasonic pulse velocity (UPV) tests were carried out on selected structural members for the delamination of cover concrete, quality and integrity assessment of concrete. Concrete resistivity, half-cell potentials and concrete powder samples were collected for corrosion assessment of rebars. Figures 1 and 2 show the concrete powder sample collection and HCP survey on a typical structural member. The test data were analysed and observed that the deteriorations such as signs of corrosion, delamination of cover concrete, cracking, seepage/leakage, loss of rebars due to corrosion, etc. are observed in some of the columns and beams of PTP and DM plant structures. Dampness and seepage of water is observed through RC walls of clarifloculators, which has to be arrested completely for long term durability against rebar corrosion.

Fig. 1 Concrete powder sample collection on a typical column

Fig. 2 Half-cell potential measurements on a typical column

aBenefits likely to accrue to the sponsor on completion of project:

Repair measures were suggested for improving the quality, integrity and durability of structural members/components, which in turn, enhance the long term durability of plant structures.

Sponsored Research Project	Wind tunnel investigations on 200m tall RC chimneys - FGD system package for RIHAND STPP, Stage II & III (4X500 MW) March 2019 - June 2019

Project Leader

Shri G. Ramesh Babu

Team

Dr A. Abraham
Smt S. Chitra Ganapathi
Smt M. Keerthana

Sponsoring Agency: M/s. Mitsubishi Hitachi Power Systems India Pvt. Ltd.

Objectives Achieved/ Progress made:

Wind tunnel investigations were carried out on two 200m tall RC chimneys under isolated and interference conditions (Fig. 1). Tests were conducted on the 1:250 scale aero-elastic model and model is instrumented with strain gauges at four different locations i.e., at base, at 0.25 H, 0.5 H and at 0.75 H to measure the bending moment at those locations and also instrumented with accelerometers at top to measure tip deflections. Tests were carried out in two sets of interference configurations for various angles of wind incidences for both shell alone and shell with flue liner cases with nine different wind speeds in the range of 15.5 m/s to 34 m/s. Based on the detailed analysis of data of all the test cases, the final design base bending moment and design tip deflections including interference effects have been determined.

Fig. 1 View of the models of chimneys with interfering bodies in wind tunnel for typical angles of wind incidence (60^0 and 330^0)

Benefits likely to accrue to the sponsor on completion of project:

Bending moments and tip deflections of the proposed chimneys considering interference effects are useful for the design of the proposed 200m tall chimneys.


SPOTlight
Structural Engineering News
& Research Updates

What could we do with bigger data pipes? Singapore tests a 5G construction site

Date: June 13, 2022

Robots and drones equipped with scanners are often held up as a productivity breakthrough for construction, allowing teams to monitor activity and measure progress automatically without requiring the physical presence of surveyors and supervisors.

But their usefulness is limited by the data-carrying capacity of today's wireless telecommunication networks, the "pipes" through which data travels.

Robots and drones may be able to collect gigabytes of data per second, but it takes a long time to send that quantity of data over the airwaves through today's fourth generation (4G) networks, meaning real-time interaction between the BIM model, say, and the new data coming in is difficult.

20,000% faster

The emerging fifth generation (5G) standard for broadband cellular networks could change that because its "pipes" are exponentially bigger.

Claims vary but according to Verizon, 4G delivers data at a rate of 100 megabytes per second while 5G can deliver at a rate of 20 gigabytes a second, a nearly 20,000% increase, meaning real-time transmission of huge amounts of data becomes possible.

What this might mean for construction is now being tested in Singapore in a pilot run by Gammon Pte Ltd, the Singaporean subsidiary of Hong Kong-headquartered Gammon Construction, mobile operator Singtel, and the Building Construction Authority, an agency of the government of Singapore.

Standalone 5G network

The trial is taking place on Sentosa island where Singtel has deployed a standalone 5G network for Gammon's site running in the 3500 MHz spectrum band. Supported by Govtech Singapore, the project is set to run until the end of 2022.

The GSMA, a global organisation representing mobile network operators, has prepared a case study of the trial to show the potential of 5G combined with mobile computing and data collection to advance construction productivity.

Four things to test

According to it, Gammon hopes to boost productivity by as much as 40% by using robots, drones and other technology in four ways. In the first, 5G-connected robots from Boston Dynamics track the progress of the structure being built. The robots use 3D laser scanners to update a building information model (BIM) residing in the cloud.

Secondly, the 5G network is used to connect to a wireless mobile CCTV station that moves around the site to transmit live video back to Gammon's command centre, where video analytics

developed by Gammon can detect hazards or breaches of safety protocol. This system spots whether a worker is wearing a hard hat or entering a restricted area, for example. Gammon bets this could reduce the number of supervisors it needs on each project.

The third use is drones equipped with a Quectel RM5000-Gl module that can inspect parts of the structure that are inaccessible without scaffolding or cherry pickers, which would speed up the inspection process and cut costs. It also opens up the possibility for future authority inspections to be conducted remotely.

Finally, Gammon is using 5G and augmented reality (AR) headsets to let workers and supervisors on site see how the planned construction methodology will unfold around them, so they can detect issues before work starts. “You start seeing potential risks that you wouldn’t see if you look just at a 3D model or step-by-step pictorials,” Michael O’Connell, general manager at Gammon, told the GSMA.

Live feed from site

The high capacity of the 5G network allows for the 3D scanning data collected by the robots to be processed live while they are still on site. “This is something that we’ve never managed before,” O’Connell said. “I wouldn’t say it’s the Holy Grail, but it is quite close.”

He added: “If I have got 50 to 60 scan points that I want to do in a day, I’d send two skilled employees down to the site to do that scanning and it would probably take them the entire day and even then I can’t process anything until they come back [with memory cards].”

The 5G-connected CCTV notifies Gammon staff immediately about any safety or operational risks. Michael O’Connell said he couldn’t quantify the benefit of that yet, but expected that the system would lead to a significant reduction in accidents.

“The 3D model tends to drift”

O’Connell approved of using augmented reality to visualise the sequence of construction on site. “The trial that we did on Sentosa was very, very successful,” he said. “You’re essentially taking an operations team or your safety team and you’re going through the step-by-step installation in

the actual location on site, a digital trial run for the upcoming activity. So we will certainly be looking at using that for some of the key risk activities on our new MRT (mass rapid transit system) project."

He also said 5G would enhance the usefulness of BIM models. "You need 5G capabilities because of the size of the data you're dealing with now with some of the BIM models, they're so detailed. If you want to use those models for verification of what you've built, then you need that 5G capability. If I want to laser scan something and overlay it for the BIM model, I can get a very accurate representation. But if you don't have the bandwidth … the 3D model tends to drift."

Story Source:

https://www.globalconstructionreview.com/what-could-we-do-with-bigger-data-pipes-singapore-tests-a-5g-construction-site/

The world's first floating city prototype unveiled in South Korea

The self sustainable city is designed to handle rising sea levels.

Date: April 27, 2022

In a response to the threat posed by rising sea levels, UN-Habitat, the Busan Metropolitan City of the Republic of Korea, and the blue tech company OCEANIX unveiled the world's first prototype sustainable floating city.

"Sea level rise poses an existential threat for some small islands and some low-lying coasts," states a recent IPCC report from February.
The climate change and information portal, run by the National Oceanic and Atmospheric Administration, Climate.gov points out that the global sea level has risen by eight to nine inches since 1880. What's more unnerving is that one-third of the rise in sea level happened in the last 25 years.

The floating city, OCEANIX Busan, aims to provide breakthrough technology for coastal cities facing severe land shortages that are compounded by climatic threats. The city will serve as the "world's first prototype sustainable floating city," aiming to be "a flood-proof infrastructure that rises with the sea," supplying its own food, energy, and water.

The floating city has six integrated systems: zero waste and circular systems, closed-loop water systems, food, net-zero energy, innovative mobility, and coastal habitat regeneration. These interconnected systems will generate 100 percent of the required operational energy on-site through floating and rooftop photovoltaic panels.

Each neighborhood will treat and replenish its own water, reduce and recycle resources, and provide innovative urban agriculture.

OCEANIX Busan is the world's first prototype of a resilient and sustainable floating community. The interconnected neighborhoods spread across 6.3 hectares that can accommodate a community of 12,000 people.

Starting from a community of 3 platforms with 12,000 residents and visitors, it has the potential to expand to more than 20 platforms. The floating platforms are accompanied by dozens of

productive outposts with photovoltaic panels and greenhouses that can expand and contract over time based on the city's needs.

Designed to meet the emerging needs of coastal cities

The designer of the city was OCEANIX, a U.S.-based blue tech company that designs and builds floating cities, while the BIG-Bjarke Ingels Group and SAMOO (Samsung Group) were the lead architects of the project.

"Today is a pivotal milestone for all coastal cities and island nations on the frontlines of climate change. We are on track to delivering OCEANIX Busan and demonstrating that floating infrastructure can create new land for coastal cities looking for sustainable ways to expand onto the ocean, while adapting to sea-level rise," said Philipp Hofmann, CEO of OCEANIX.

"As Mayor of the Metropolitan City of Busan, I take seriously our commitment to the credo 'The First to the Future'. We joined forces with UN-Habitat and OCEANIX to be the first to prototype and scale this audacious idea because our common future is at stake in the face of sea level rise and its devastating impact on coastal cities," said Busan Mayor Park Heong-joon, who has set an ambitious agenda, including turning Busan into a green smart city and launching a bid for World Expo 2030.

The Executive Director of UN-Habitat, Ms. Maimunah Mohd Sharif said, "We cannot solve today's problems with yesterday's tools. We need to innovate solutions to global challenges. But in this drive for innovation, let's be inclusive and equitable and ensure we leave no one and no place behind. I am happy this Roundtable takes place ahead of the High-Level Meeting on the New Urban Agenda, where cities and countries around the world come together to discuss sustainable urbanization."

"In designing a solution for the most vulnerable coastal locations on the frontlines of climate change, OCEANIX's new modular maritime neighborhoods will be a prototype for sustainable communities informed by Busan's unique juxtaposition of old and new. Creating a connection

between the city and the seaside, OCEANIX Busan will expand this spirit onto the waterfront," said Bjarke Ingels, Founder and Creative Director of BIG-Bjarke Ingels Group.

This is as scary as it is exciting to achieve such a feat, but living in a city that resembles the communities where people try to survive in the dystopian movie *Water World* is kind of pessimistic.

Story Source:

https://interestingengineering.com/the-worlds-first-floating-city-prototype-unveiled-in-south-korea

---


PRODUCTS
&
APPLICATIONS
Updates

Applying Artificial Intelligence to Construction

Rene Morkos is the founder and CEO of ALICE Technologies, which is the industry's first AI-powered simulation and optimization platform for construction planning, scheduling, and management. Born the son of a civil engineer, Rene was raised in the construction business. And, as an adult, Rene Morkos has worked on projects large and small that span across the globe including places such as: Beirut, Dubai, Afghanistan, and Athens. No matter where he went, however, the same questions plagued every jobsite on every continent: "How do we build faster?" "What can we do to speed up the job?" "Why are crews waiting?"

The answer came to Rene when he was researching during his PhD in Construction Management at Stanford; the research revealed that on any given construction site, work was only being completed 3 percent of the time. Morkos describes this moment as an "epiphany" and made him wonder what he could do to make the construction industry more efficient and more effective. Stanford's location at the heart of Silicon Valley gave him inspiration on where to start.

Morkos soon began researching ways in which artificial intelligence (AI) could play a role in addressing the construction industry's inefficiencies. The result was an application of AI to construction scheduling and ongoing project management. Thus, ALICE Technologies was created.

Now, ALICE has evolved into a tool that helps contractors and owners plan, bid, and build more effectively, focusing primarily on the infrastructure segment. The technology is so effective, in fact, that for a typical $500 million dollar construction project ALICE cuts the project duration by an average of 15 percent and reduced labor costs by an average of $30 million.

ALICE is able to do this because it does what no human can do, generate millions of potential scheduling options within minutes. It also allows owners and operators to analyze and choose which of these scheduling options works best for them. This becomes even more prescient when projects are delayed or altered by unforeseen circumstances—global pandemic, delayed shipments, extreme weather, etc.—that have the potential to slow construction and raise both material and labor costs.

ALICE is simple to use as well, requiring only that users upload a 3D model, break down scope, input construction methods and cost information, and add addition constraints. Within ten minutes of setting the plan, ALICE generates a multitude of valid resource-loaded solutions for building and optimizing resources. This helps contactors manage risk, selecting the best strategy and schedule for their project. Knowing that they have covered all major contingencies also helps contractors bid more confidently because they know their proposal is not only constructible but is also optimized to their goals.

For now, ALICE has primarily found a home in larger markets, serving big companies—such as Parsons, HDCC, and Kajima Corporation—that work on big projects. Morkos also believes there is a ton of room to grow. He notes that much of the technology within the same sector—Excel, Microsoft Project, and P6—was developed decades ago and are still being used. He believes that ALICE represents a powerful new alternative to these old methods. The key now, according to

Morkos, is helping the market understand how to put these alternatives to work and make it easier for customers to embrace and use them.

Improve project schedules, find your optimal resource mix, and maximize project profitability with ALICE

Deliver better business results with the world's first AI-powered construction simulation and optimization platform.

Simulate multiple construction strategies in minutes

With ALICE, you can explore multiple construction options to help you reduce your costs and build faster. Optimize key project resources like labor, equipment, and materials. And because ALICE is parametric, any changes you make flow immediately throughout your schedule.

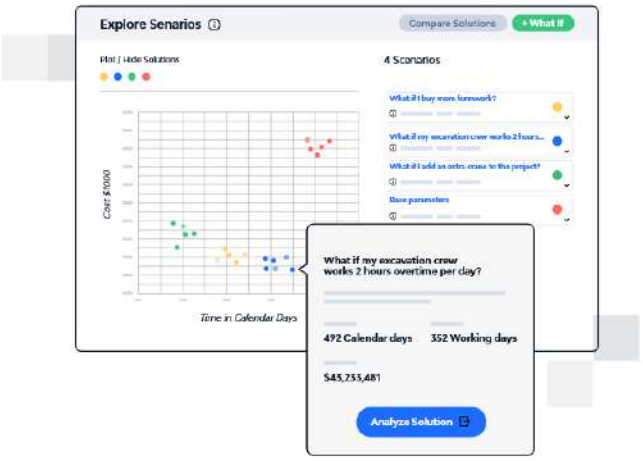

Digitize your construction methods

ALICE Recipes contain the construction tasks that guide your project plan. Use them to digitize your company's unique methods and transfer key learnings from project to project so you never have to start planning from scratch or create schedules manually.

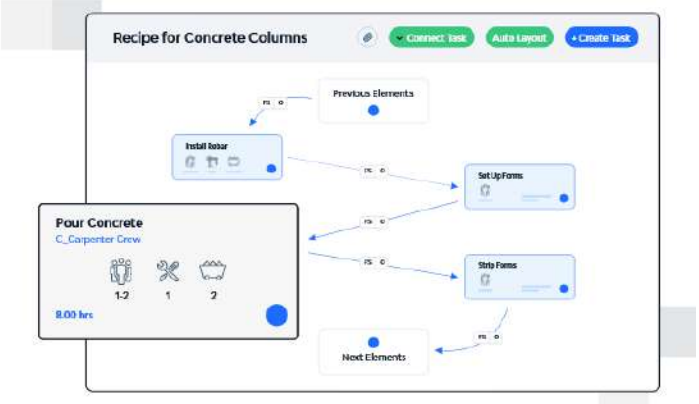

Source: https://blog.alicetechnologies.com/case-studies/airport-expansion-project

Overcoming Complexity and Driving Efficiency in Bridge Design with Parametric Design

Engineers are under growing pressure to be more productive while, at the same time, structural design is becoming increasingly complex. The architectural design tools of today have expanded the possibilities for more curves and amazing structural details, all of which end up on the desktops of structural engineers who are working with smaller budgets to meet tighter deadlines. While this is especially true in bridge design, the majority of the bridge industry remains heavily reliant on drawings as primary documents. Although widely adopted, traditional 2D CAD workflows don't solve the challenges commonly seen on projects today such as material waste, rework, RFIs, budget overruns, schedule delays, and a general lack of productivity.

These constraints are driving a growing number of structural engineers to explore parametric design and BIM-based workflows. Parametric design shifts the expression of design from geometry to the underlying logic, allowing engineers to establish rules and parameters for a model, rather than model the geometry directly. These rules operate on the input parameters, and the model is an inevitable outcome. So, when adjusting one parameter, such as the number of columns or the width of a deck, all of the model objects affected by that change are automatically updated. When parametric design is combined with the proper BIM software, the parameters can simultaneously drive information-rich BIM data beyond simple geometry.

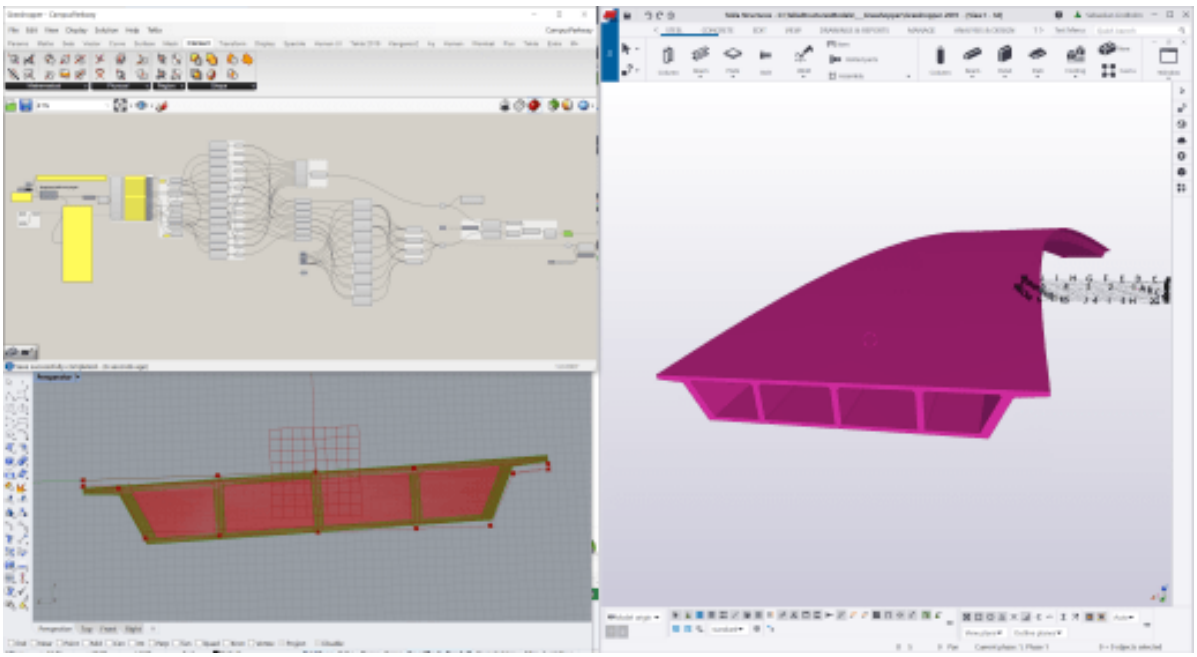

This might sound complicated, but it's all about overcoming limitations and rapidly creating design alternatives for complex shapes. Today, structural engineers are leveraging a parametric workflow without prior knowledge of programming through direct links between BIM software and visual programming tools such as Grasshopper, a pre-installed plugin for Rhinoceros 6, a 3D computer graphics and computer-aided design (CAD) application. This allows engineers to define input parameters such as coordinates, dimensions, or curves and visually script rules that act on those parameters, generating the desired geometry or other output, which can then be applied

directly to live objects using a parametric BIM software. By bringing the parametric design into a 3D parametric modeling environment, such as Tekla Structures, repetitive tasks and change updates are automated. This allows engineers to quickly, accurately and easily create a truly constructible 3D bridge model, fulfilling any Level of Development (LOD) requirement and ensuring all deliverables, including the model, drawings and material lists, are consistent.

Based on attributes the engineer defines, the effects of any change to the design are automatically populated throughout the model. Grasshopper takes the inputs, completes the calculations, and produces an output that is applied to the model. This eliminates the need to manually apply changes across the model and allows engineers to quickly generate and visualize multiple iterations of complex designs in 3D by simply adjusting the attributes. This workflow is especially beneficial when modeling structures, such as bridges, that have complex geometries and curved surfaces.

The Many Benefits of Parametric Design

Modeling with parametric design has significant benefits that improve both the design process and quality. With architects pushing the boundaries of design and projects becoming increasingly collaborative, eliminating manual processes can help structural engineers work more efficiently to meet today's project demands. By combining parametric design with parametric modeling, engineers can:

- **Accelerate work and increase accuracy.** Parametric design lets engineers define logical rules describing the model and the relationships between its parts, as well as a set of parameters to drive the logic. The design tool then calculates and creates a dynamic 3D model based on that criteria that, when used with a parametric BIM software such as Tekla Structures, leads to a detailed, data-rich constructible model that contains all the information needed to build and fabricate. Eliminating manual work provides a tremendous productivity advantage by accelerating model creation and the automatic generation of the design as a whole decreases the chance for human errors that can, at worst, accumulate into costly miscalculations.
- **Simplify iterations.** Addressing changes is much easier with parametric modeling than with a traditional 3D model, not to mention 2D CAD. Because adjustments to the model are based on the set logic and reflected throughout the entire design, it's possible to iterate quickly while staying within a design's established criteria and constraints.
- **Innovate with ease.** When the entire design can be created, managed and iterated as a whole, there are more opportunities to optimize the design process. Parametric design and modeling provide engineers with an easy way to rapidly test and discover options for making a project more cost-effective. When a better option is discovered, the changes can be implemented quickly and with ease.

Getting Started

Trying a new approach or workflow for the first time can be intimidating. To give parametric design a try, consider these four steps:

1. **Be willing to try something new.** This may seem obvious, but it would be easy to read the word parametric and think, "this is too complicated" or "I'm not a programmer and I don't have time to learn something new." If you want to give parametric design a try, the full version of Rhino Grasshopper is free to evaluate for 90 days. What's the harm in trying it out?
2. **Take advantage of tutorials and instructional videos.** The best way to learn is online through videos made by other structural engineers, tutorials, and forums. Some personal favorites: Grasshopper-Tekla Structures demo, Grasshopper basics and these tutorials. It's also fun to

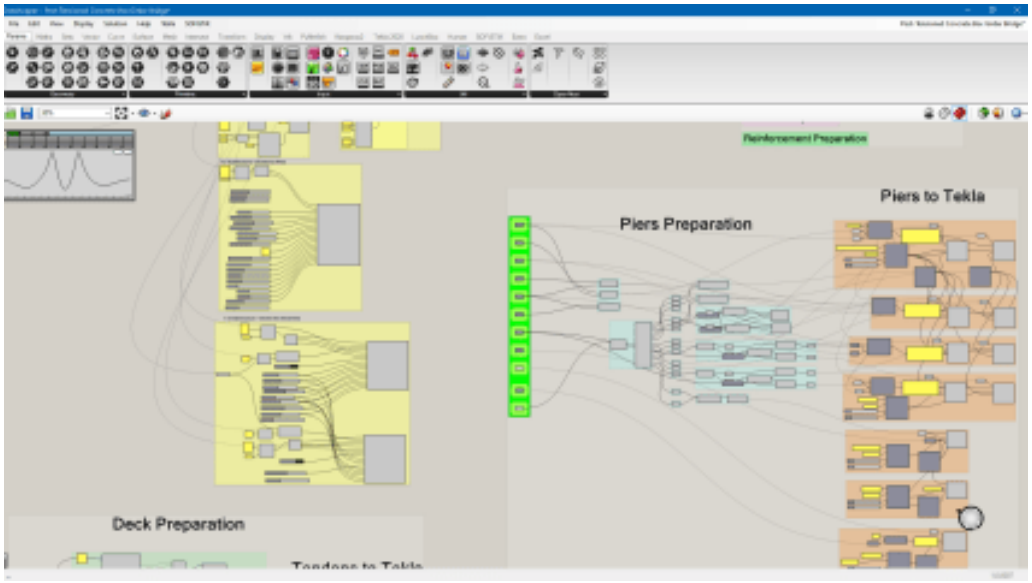

   experiment with sample Grasshopper scripts which can be found with a simple Google search.
3. **Experiment with a simple design.** Start by experimenting with parametric data for a simple design in Grasshopper and create output objects in a parametric BIM software. It's not necessary to jump right in and learn using a complex bridge model. For example, build a simple wireframe structure, such as a portal frame, and use the line output as centerlines for the parametric BIM objects.
4. **Get Organized.** It's important to know that parametric design and modeling require organization. Create notes and keep the script of parameters organized and well documented so that any project stakeholder can understand it a week, or even a month, later.

With dynamic automation, increased accuracy, rapid iterations, and more resources for the design as a whole, the benefits of parametric design are undeniable. While it can be used for any project big or small, it's especially advantageous in complex structures with unconventional architecture. Using parametric design with constructible BIM-tools takes the modeling process to the next level and makes it possible to streamline work, create high-quality and constructible designs and deliver successful projects – totally model-based without drawings.

Source: *https://csengineermag.com/overcoming-complexity-and-driving-efficiency-in-bridge-design-with-parametric-design/*

Concrete Protective Liner by Russian company Hydropolymer

Concrete protective liner is a multipurpose solution for waterproofing and protection of concrete surfaces against corrosion and destruction. The product warranties long-term and reliable protection of structures under extreme operating conditions. It is manufactured using high quality raw materials: PP, PE, LDPE, and HDPE. Russian company JSC Research and Development Enterprise Hydropolymer is specialized in production of Concrete Protective Liner (CPL) made of polyethylene and polypropylene with anchor ribs in order to protect multipurpose building structures as well as in manufacturing lined reinforced concrete elements.

Lining using a polymer sheet prevents concrete corrosion, thereby expanding the structure's service life. The unique system of anchor ribs ensures maximum adhesion of polymer sheet with the concrete structure. Absolute density of seam welding prevents infiltration and exfiltration and contributes to environmental protection.

Looking at the benefits of Concrete Protective Liner, it is the ideal solution for surface protection and leak proofing the substrate because of its low total cost of ownership to the end client and long-term protection. In comparison with CPL, GRP Lamination has difficulty in doing high quality surface preparation followed by lamination, which is totally dependent on the quality of workmanship. Regarding different paintings and coatings, they need very high maintenance due to their very nature and therefore are an expensive and short-term option considering the life of the asset.

Advantages of Concrete Protective Liner

- Outstanding chemical resistance (absence of corrosion caused by water, alkali, acids and gas)
- Cracking and heat-ageing resistance
- Elasticity (resistant to considerable deformations)
- Reduction of operation costs (lifespan of 50 years as minimum, maintainability)
- Environmentally friendly
- Wide range of applications in concrete structures
- Absolute mechanical anchorage in concrete
- Simple and safe installation
- High impact resistance
- Absence of voids upon molding of products and installation of the sheet
- Wide range of temperatures (-20 up to + 90° C)
- Reduction of abrasive wear
- Increased flow laminarity
- Meets hygiene and potable water requirements

Application

- Precast concrete manholes
- Precast concrete pipes and jacking pipes
- Irrigation
- Water treatment
- Potable water tanks
- Refurbishment of existing structures

Source: https://www.nbmcw.com/product-solutions/concrete-chemicals-waterproofing-repairs/waterproofing-construction-chemicals/concrete-protective-liner-by-russian-company-hydropolymer.html

Agru Suregrip Protective Lining

At Forterra we take pride in our ability tobring our customers the affordable, quality construction materials they need. Providing pre-fabricated designs that save time andmoney while increasing safety is one of many ways we do just that.Agru SureGrip®Concrete Protective Liner Agru SureGrip® Concrete Protective Liner offers unbeatable protection for almost any application. It not only protects concrete from bacterial and chemical damage, it's 100% gas- and watertight to eliminate inflow and infiltration. It's perfect for manholes, wetwells, treatment plants and other challenging environments. To learn more about how Agru SureGrip®Concrete Protective Liner can help you keep things flowing smoothly, talk to Forterra today. Applications

- Agru SureGrip® Concrete Protective Liner contains the following innovations
- 39 studs per square foot guarantee the best possible anchorage between the concrete and liner• Back pressure resistance: HDPE 67 ft. (29 psi)•
- 600% elasticity• Shear resistance per stud: 4,500 lbs•

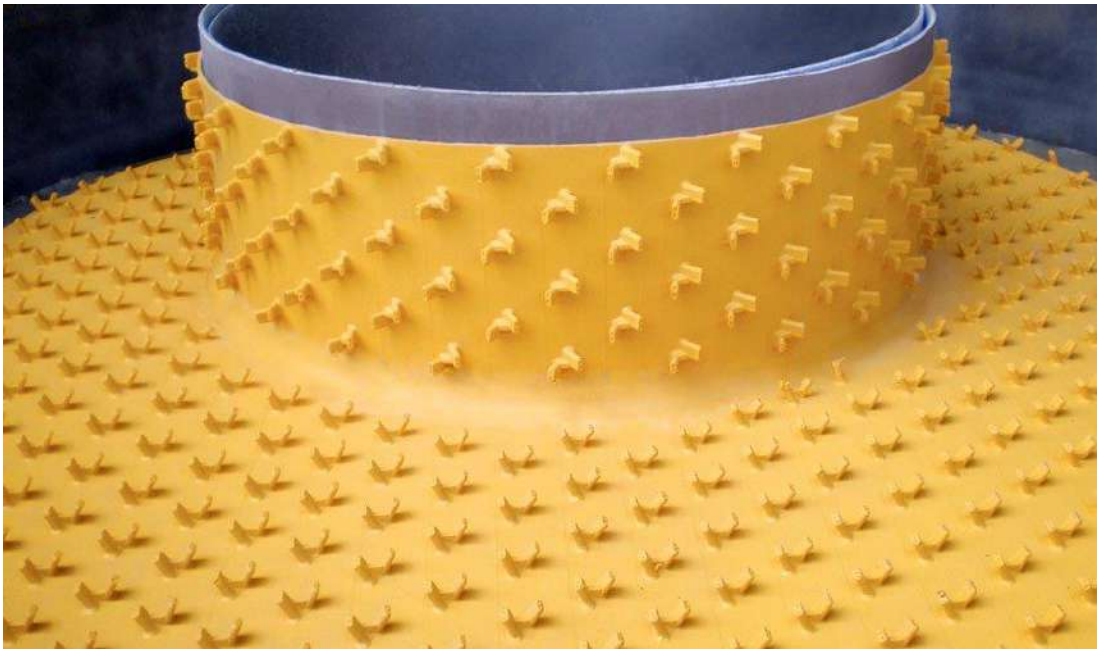

- High pullout resistance: 112 lbs. per stud• 2mm thickness for wastewater applications• 3mm or 5mm thickness available for industrial and landfill projectsProduct BenefitsFactory-welded penetrations provide unmatched protection:•
- The ultimate concrete protection from bacterial and chemical attack•
- The liner is 100% impermeable to gas and water• Extends service life of wastewater systems•
- Agru certified field welding and spark testing required•

- Agru SureGrip® Concrete Protective Liner extends the design life of the host structure• HDPE welding fumes are nontoxic
- Typical Applications Agru SureGrip®Concrete Protective Liner:• New Sanitary Manholes• Industrial Manholes• Landfill Collection Structures• Wastewater Treatment Plants• Wetwells, Vaults and Pipe• Rehab Existing Concrete Structures• Other Challenging Environments

Pipe connections require no further field welding. Lined boot openings ensure a gastight seal at all pipe entries. No further fieldwork is required.

Source: https://www.forterrabp.com/protective-lining-systems-agru-suregrip/

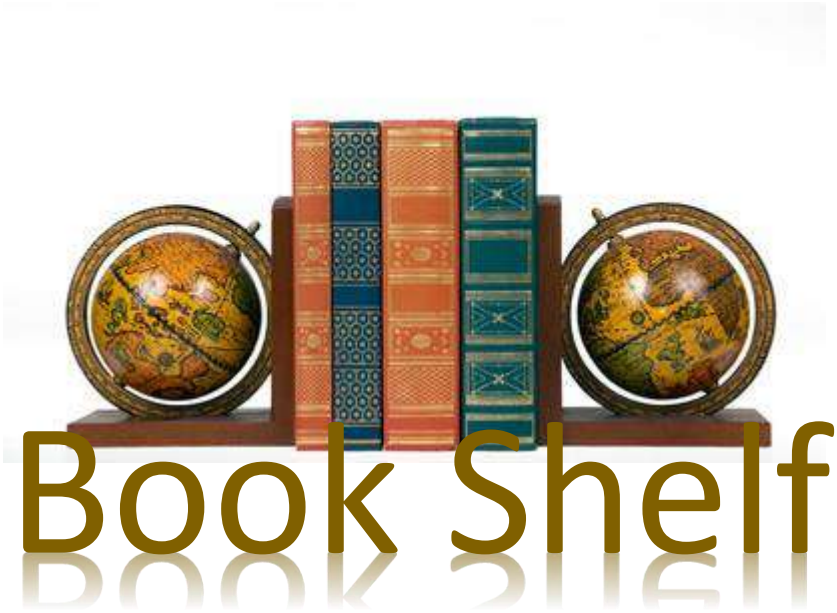
Book Shelf

Vibration Mitigation Systems in Structural Engineering

Edition: 1
Author: Okyay Altay
Publisher: CRC Press
ISBN: 9781138564169
Year of publication: 2022

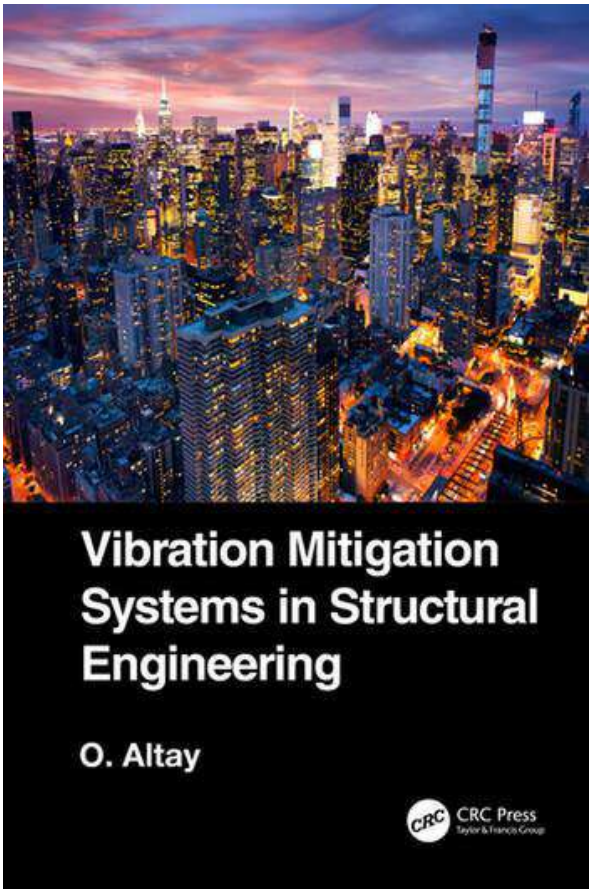

Description

The scope of the book is the application of vibration mitigation systems in structural engineering. The intended content includes the theoretical background covering aspects from both structural dynamics and control engineering point of view. Moreover, passive, active and semi-active devices are explained in detail giving mathematical principles, design considerations and application examples. It also contains detailed information about structural monitoring, as an essential part of the active/semi-active systems, and therefore, provide a full overview about passive, active and semi-active systems in the specific context of civil engineering

1. Book presents a comprehensive coverage of the area of vibration control of civil structures subjected to different types of loading while using passive, semi-active, and/or active controls.

2. Presents the theoretical governing equations as well as the associated design guides of various vibration control mitigation approaches.
3. Discusses structural monitoring aspects such as sensor technology, system identification and signal processing topics.
4. Reviews structural control aspects, such as algorithms.
5. Includes solved examples utilizing MATLAB®/SIMULINK® with source codes of the calculation examples and design tool set.

This book is aimed at graduate students, professionals, researchers in civil engineering, structural engineering, structural dynamics, health monitoring, vibration control.

Numerical Models for Vehicle-Bridge Interaction Dynamic Analysis
with the application in highway and railway bridges and high-speed trains

Edition: 1
Author: Hossein Azimi
Publisher: LAP Lambert Academic Publishing
ISBN: 9783659407802
Year of publication: 2013

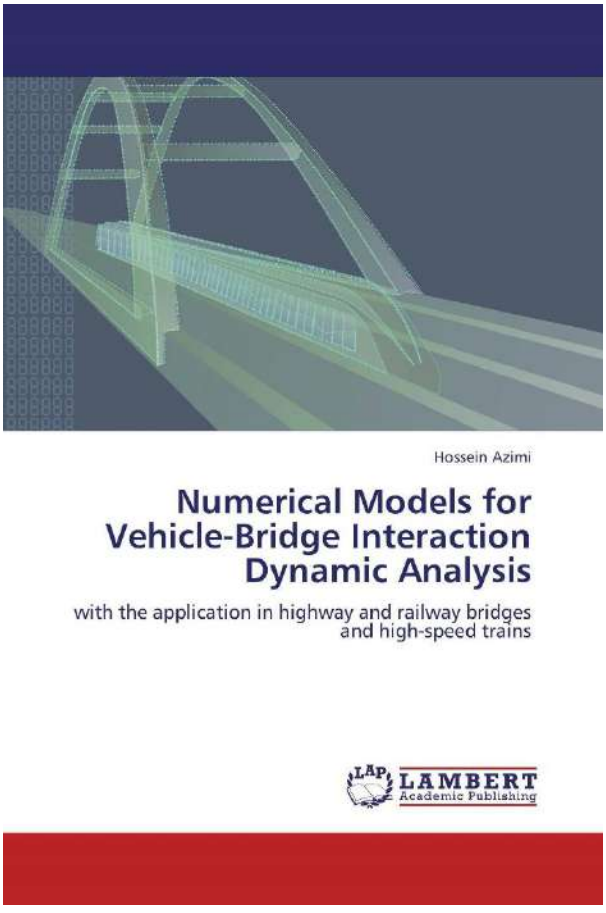

Description

The main objective of this book is to establish efficient numerical models within the framework of finite element method to solve the dynamic response of the Vehicle-Bridge Interaction (VBI) systems for vehicles moving with constant velocity or with acceleration. For vehicles with constant velocity, the dynamic condensation method is applied to reduce the vehicle DOFs to the VBI element. VBI element refers to bridge beam elements that are in direct contact with wheels of the vehicles traversing the bridge. A new formulation is proposed for the mass, damping, and stiffness of the VBI element considering new formulation for the contact points. For vehicles experiencing sudden deceleration with sliding, external forces resulting from vehicle horizontal deceleration are numerically formulated in a matrix form as the function of vertical contact forces. By defining a new parameter called acceleration parameter with particular characteristics, the contact force formula is reformulated. Consequently, a new formulation for the VBI element containing the effect of vehicle acceleration is developed.

FOR MORE DETAILS

Head, Knowledge Resource Division
CSIR-Structural Engineering Research Centre,
CSIR campus, Taramani, Chennai 600113
Phone : 044-22549131 / 132 / 133
Fax : 044-225491508
Email : liba@serc.res.in

READ
RESEARCH
WRITE
REPEAT